Radiation

&EPA
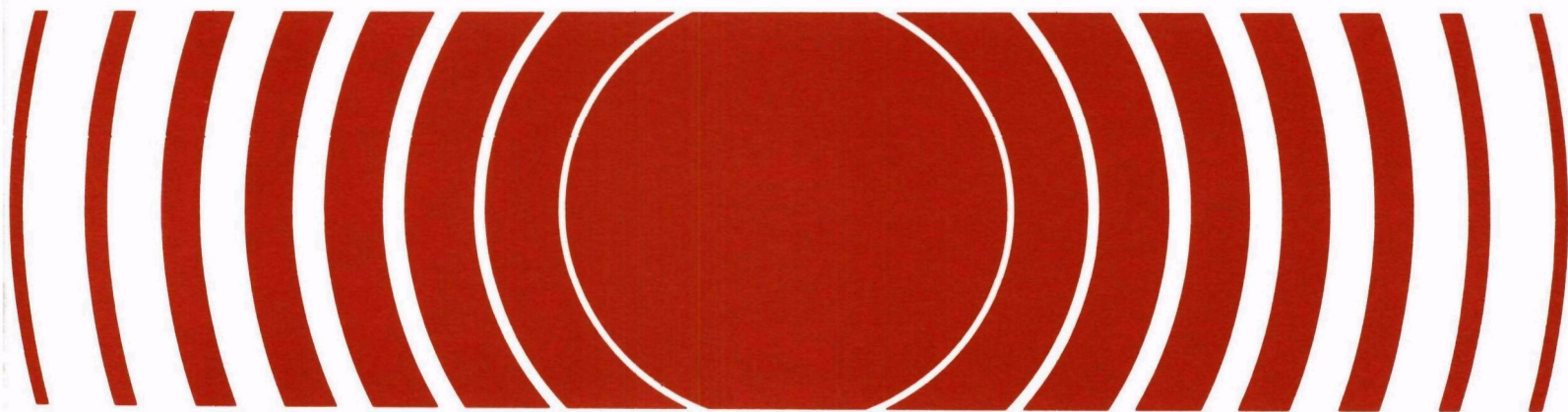
Technical Support of Standards for High-Level Radioactive Waste Management

Addendum to Volumes C and D

TECHNICAL SUPPORT OF STANDARDS FOR

HIGH-LEVEL RADIOACTIVE WASTE MANAGEMENT

ADDENDUM TO VOLUMES C AND D

EPA Contract No. 68-01-4470

Prepared by

Arthur D. Little, Inc.
Cambridge, Massachusetts   02140

March 1982

DISCLAIMER

This report was prepared as an account of work sponsored by the Environmental Protection Agency of the United States Government under Contract No. 68-01-4470. Neither the United States nor the United States Environmental Protection Agency makes any warranty, express or implied, or assumes any legal liability or responsibility for the accuracy, completeness, or usefulness of any information, apparatus, product, or process disclosed, or represents that its use would not infringe privately owned rights.

ACKNOWLEDGMENTS

FOREWORD

A major Federal effort is underway to develop methods for disposal of high-level radioactive waste in deep geologic repositories. An important element of this program is the development and promulgation by the U.S. Environmental Protection Agency (EPA) of environmental standards for the management of these wastes.

In anticipation of its efforts to develop these standards, EPA recognized that it would be necessary to estimate the expected and potential environmental impacts from potential geologic repositories using modeling techniques based upon as thorough an understanding as possible of the uncertainties involved in the quantities and characteristics of the wastes to be managed, the effectiveness of engineering controls, and the potential migration and accidental pathways that might result in radioactive materials entering the biosphere. Consequently, in March 1977, the EPA contracted with Arthur D. Little, Inc., for a study to provide a technical support for its development of environmental regulations for high-level radioactive wastes. This study was divided into the following four tasks:

Task A - Source Term Characterization/Definition

Task B - Effectiveness of Engineering Controls

Task C - Assessment of Migration Pathways

Task D - Assessment of Release Mechanisms

Since the completion of these reports several years ago, research by many organizations has been proceeding at a very rapid rate, and thus it is of interest to determine to what extent the contents or conclusions should be updated. In particular, the purpose of this report is to examine several issues relevant either to the conclusions of Tasks C and D or to their subsequent use by EPA and others, and to identify additions or modifications that may be dictated by such additional data and analysis. The ten major sections are essentially independent of each other, but are often dependent on further background information from the Task C and D reports.

TABLE OF CONTENTS

LIST OF TABLES

LIST OF FIGURES

1. FREQUENCY OF FAULT MOVEMENT

The values for frequency of fault movement used in the analyses presented in the Task D Report were based on an estimate of the time since the most recent movement along existing faults. The equations used to calculate first-estimate fault frequency and second-estimate fault frequency were $\lambda = 4/N$ and $\lambda = 10/N$, respectively, where λ is the fault failure rate (events/year), N is the time since the most recent fault movement (years), and the constants are based on estimates of fault frequency within the area of the repository. The fault failure rates used in the Task D Report analyses are given in Table 1-1.

The purpose of this section is to review the previous estimates in light of more recent data from certain regions with characteristics similar to those assumed for the generic repositories in the Task D Report. Only salt formations are considered, since these are the formations for which new data have appeared. This review lends support to the first-estimate values used in the Task D Report, but it suggests that second-estimate values should be higher. It should be emphasized that even though real data are used for these calculations, the resulting numbers should not be interpreted as applying to the specific sites. It is outside the scope of this study to estimate fault movement probabilities for specific regions or sites. Such estimates would be expected to be based on more extensive data and a detailed analysis of geologic processes at the site.

1.1 PARADOX BASIN

The 1982 geologic characterization report (Woodward-Clyde, 1982) for the Gibson Dome area of the Paradox Basin indicates that major faulting occurred during Late-Cretaceous and Cenozoic time (approximately 65 to 10 million years before present [MYBP]) as a result of regional tectonic forces. There is also scattered

TABLE 1-1

VALUES FOR FAULT MOVEMENT FREQUENCY

USED IN TASK D REPORT ANALYSES

	First Estimate (events/year)	Second Estimate (events/year)
Bedded Salt	2×10^{-8}	4×10^{-7}
Granite	2×10^{-8}	10^{-5}
Basalt	5×10^{-7}	10^{-5}
Shale	2×10^{-8}	4×10^{-7}
Dome Salt	3×10^{-7}	10^{-5}

evidence of Quaternary faulting (less than 2 MYBP), but the general lack of Quaternary cover makes it difficult to assess and date the most recent episode of faulting. Using both 65 and 10 MYBP in first-estimate calculations yields a fault movement frequency of 4 x 10^{-7} to 6 x 10^{-8} events/year. Using 1 MYBP as a conservative value i.e., tending to overestimate the risk, for second-estimate calculations yields a fault movement frequency of 10^{-5} events per year.

1.2 PERMIAN BASIN

The area geologic characterization report for the Palo Duro and Dalhart Basins of Texas (Stone and Webster, 1981) contains a summary discussion and a table of fault data. Most of the faulting has been described as Late Mississippian to Early Permian in age and does not affect the overlying salt strata. Two faults, however, with as much as 600 feet displacement, are reported to intersect the upper Permian salt strata. Relative age dating on the basis of stratigraphic relationships indicates that the most recent movement along these faults occurred during Late Permian (approximately 250 MYBP) and Triassic (approximately 225 MYBP). Using these data would result in fault movement frequencies of 1.6 to 1.8 x 10^{-8} events/year.

1.3 GULF COAST REGION

The geologic characterization reports for the Mississippi and Louisiana study areas of the Gulf region (Law Engineering, 1980) identify several faults that were active during Late Jurassic (approximately 140 MYBP) and Late Cretaceous (approximately 65 MYBP) time. The report for the Mississippi study area also states that interpretation of seismic data indicates that there has been no post-Eocene (approximately 40 MYBP) fault movement that could affect the proposed host rock. Investigations are being undertaken, however, to evaluate what is believed to be relatively shallow faulting that has occurred in the Quaternary (less than 2 MYBP). Using the Late Jurassic to Eocene dates for first-estimate

calculations and 1 MYBP for second-estimate calculations yields fault movement frequencies of 1.0 to 2.8 x 10^{-7} events/year to 1 x 10^{-5} events/year, respectively.

1.4 SUMMARY

On the basis of the estimates given above, there is no reason to revise the first-estimate values for faulting from those given in Task D. It does appear, however, that the second-estimate values should be increased to 10^{-5} events/year. The modified values are given in Table 1-2. Second-estimate comparisons among media could be misleading if based on the new salt values and other values from Table 1-1, since more detailed study of potential sites with other host rock formations might similarly lead to higher values.

TABLE 1-2

MODIFIED FAULT MOVEMENT FREQUENCIES FOR SALT[*]

	First Estimate (events/year)	Second Estimate (events/year)
Bedded Salt	2×10^{-8}	10^{-5}
Dome Salt	3×10^{-7}	10^{-5}

[*]Note: Only the second estimates have been modified from Task D values.

References

Law Engineering Testing Company. Geologic Area Characterization. Volume 1: Introduction, Background and Summary. Gulf Coast Salt Domes Project. Prepared for Battelle Memorial Institute. August 29, 1980.

Stone and Webster Engineering Corporation. Area Geological Characterization Report for the Palo Duro and Dalhart Basins, Texas. Prepared for the Office of Nuclear Waste Isolation. December 1981. ONWI-292.

Woodward-Clyde Consultants. Geologic Characterization Report for the Paradox Basin Study Region Utah Study Areas. Prepared for Battelle Memorial Institute Office of Nuclear Waste Isolation. January 1982. ONWI 290.

2. EFFECTS OF SALT DISSOLUTION ON GROUNDWATER FLOW

For the evaluation of generic salt repositories, the analyses of groundwater flow and travel times contained in the Task D Report assumed that there were no changes in water density caused by salt dissolution. The initial analyses for the reference bedded salt and salt dome repositories are reevaluated in this section under the assumption that a breach through the repository that intersects overlying and underlying fresh-water aquifers would allow for salt dissolution that, in turn, would increase the water density. This density increase can either reduce the upward water flow rate or even reverse the direction of the flow. Sample calculations are given to show this effect. Naturally, the importance of this phenomenon depends in part on the initial degree of salinity of the water that could flow through a pathway. Many deep groundwaters in salt regions are already quite saline, thereby diminishing the effect.

Tables 2-1 and 2-2, which are taken from the Task D Report, summarize the effective hydraulic gradients used to analyze flow rates in boreholes and faults in bedded salt and salt dome repositories, respectively. (These cases are chosen as examples.) Figures 2-1 and 2-2 are schematics of these reference repositories.

The gradients listed in these tables are equivalent to the head difference between the overlying and underlying aquifers divided by the vertical distance between the two aquifers. For the reference bedded salt and salt dome repositories, the aquifers are separated by a vertical distance of 200 meters and 330 meters, respectively. The Task D analyses were based on the conservative assumption that the head in the lower aquifer was greater than the head in the upper aquifer and that groundwater flow was from the lower to the upper aquifer. Tables 2-3 and 2-4 list the relative head differences that would exist between the two aquifers based on gradients listed in Tables 2-1 and 2-2.

TABLE 2-1

EFFECTIVE VERTICAL HYDRAULIC GRADIENT IN PERMEABLE BOREHOLES
(BEDDED SALT REPOSITORY)

| | Hydraulic Gradient, i | | |
	100 Years*	1000 Years	10,000 Years
First Estimate	0.13	0.11	0.04
Second Estimate	0.62	0.60	0.53

*Years after repository closure.

Source: Table D-53, Task D Report.

TABLE 2-2

EFFECTIVE VERTICAL HYDRAULIC GRADIENT IN A FAULT
(SALT DOME REPOSITORY)

	100 Years*	1000 Years	10,000 Years
First Estimate	0.13	0.08	0.04
Second Estimate	0.32	0.27	0.23

*Years after repository closure.

Source: Table D-97, Task D Report.

Surface

Surface
Deposits

Aquifer   330 Meters
                                           360 Meters
Shale
                                           410 Meters

Salt   ◄─ Repository   460 Meters

                                           510 Meters
Shale
                                           560 Meters
Aquifer
                                           590 Meters

Basement
Complex
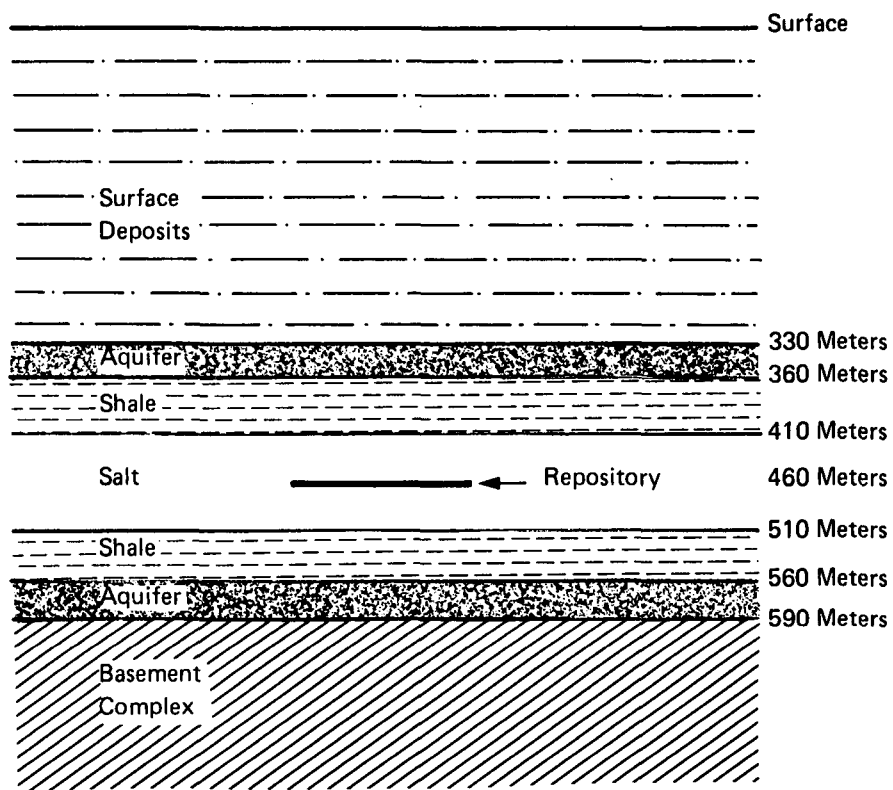
Source: Task D Report, Figure D-2.

FIGURE 2-1   REPOSITORY IN BEDDED SALT

Surface

Surface
Deposits

Aquifer

Country
Rock

Caprock

Repository

Aquifer

Salt

200 Meters
230 Meters

460 Meters

560 Meters
590 Meters
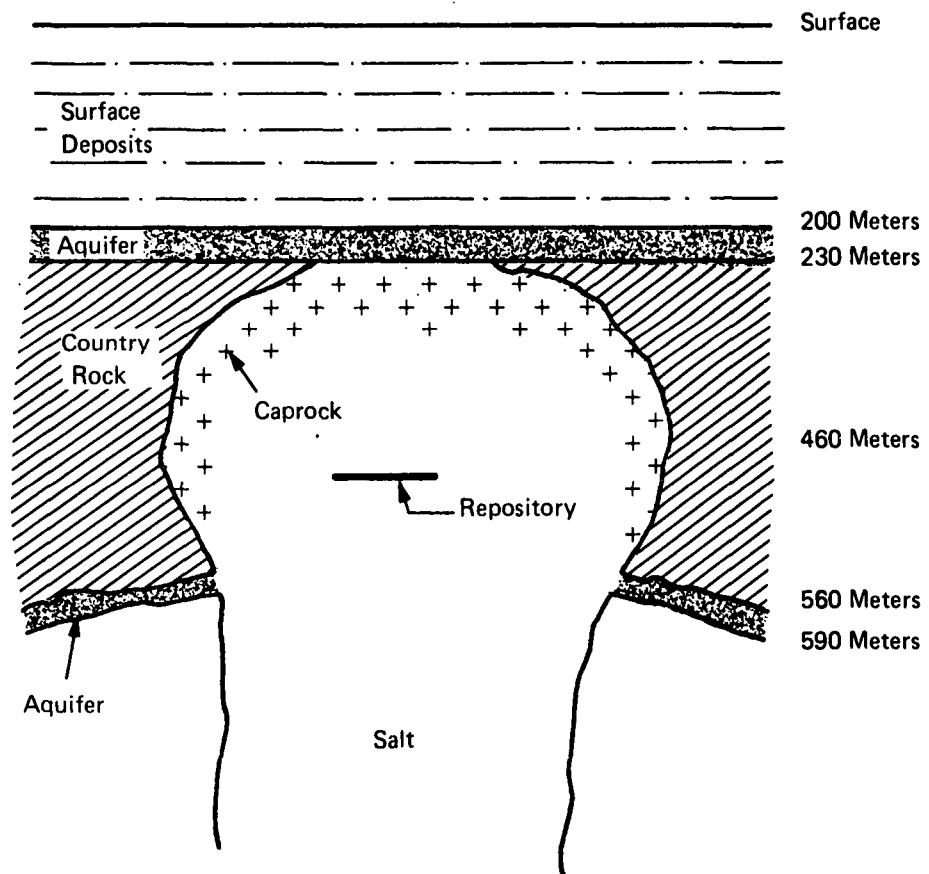
Source: Task D Report, Figure 8.

FIGURE 2-2   REPOSITORY IN SALT DOME

11

TABLE 2-3

HEAD DIFFERENCES BETWEEN THE UNDERLYING AND OVERLYING AQUIFERS
CORRESPONDING TO HYDRAULIC GRADIENTS LISTED IN TABLE 2-1
(BEDDED SALT REPOSITORY)

	Water Level Difference, Meters[*]	
	1000 Years	10,000 Years
First Estimate	22	8
Second Estimate	120	106

[*]Note: Freshwater equivalent difference

TABLE 2-4

HEAD DIFFERENCES BETWEEN THE UNDERLYING AND OVERLYING
AQUIFERS CORRESPONDING TO HYDRAULIC GRADIENTS LISTED IN TABLE 2-2
(SALT DOME REPOSITORY)

	Water Level Difference, Meters*	
	1000 Years	10,000 Years
First Estimate	26.4	13.2
Second Estimate	89.1	76

*Note: Freshwater equivalent difference

13

If a borehole or a fault were to provide a pathway from the underlying aquifer to the overlying aquifer, then fresh water could flow through and dissolve part of the salt formation. This process would change the density of the water as it flowed to the overlying aquifer.

To evaluate the effect of changes in water density caused by salt dissolution, it is necessary to evaluate the effect of the denser water on the hydraulic gradient between the underlying and overlying aquifer. The density of waters associated with salt deposits ranges between 1.027 g/cm^3 and 1.345 g/cm^3 with an average density of 1.15 g/cm^3 (Muller et al., 1981, Table 3). The present analyses assume an average density of 1.15 g/cm^3.

The change in the height of a water column, owing to a change in water density, can be calculated by the equation

$$\frac{h_s}{h_f} = \frac{\rho_f}{\rho_s} \qquad (2.1)$$

where

h_s = Height of the column of saline (denser) water

h_f = Original height of the column of fresh water

ρ_f = Density of the fresh water

ρ_s = Density of the saline water

For the present reference calculations, the correction factor for the change in height of the water column is 0.87, i.e., 1.0/1.15. This means that if a fresh water column extending from the lower aquifer to some point above the upper aquifer and with a pressure ρ_b at the bottom were replaced by a column of water also with pressure ρ_b at the bottom, but with a length L of saline water (ρ_s = 1.15) contained within it, the height of the second column of water would be 0.13 L (1.00 - 0.87) less than the height of the first column of water. Using this factor results in a head correction value of 20

meters for the bedded salt repository and 43 meters for the salt dome repository.

Tables 2-5 and 2-6 list the revised water level differences between the underlying and overlying aquifers attributable to the effects of increased density of the water between the bottom of the host salt unit and the overlying aquifer. For most of the first-estimate calculations, the effect of the increased water density is to reverse the gradient and to cause water to flow down from the upper aquifer to the lower aquifer.

TABLE 2-5

WATER LEVEL DIFFERENCES BETWEEN HYPOTHETICAL WELLS
IN THE UNDERLYING AND OVERLYING AQUIFERS CONSIDERING
THE EFFECTS OF SALT DISSOLUTION ON WATER DENSITY
(BEDDED SALT REPOSITORY)

	Water Level Difference, Meters*	
	1000 Years	10,000 Years
First Estimate	2	-12
Second Estimate	100	86

*Minus sign (-) means water level in upper aquifer is higher than
in lower aquifer, implying a downward gradient.

TABLE 2-6

WATER LEVEL DIFFERENCES BETWEEN HYPOTHETICAL WELLS
IN THE UNDERLYING AND OVERLYING AQUIFERS CONSIDERING
THE EFFECTS OF SALT DISSOLUTION ON WATER DENSITY
(SALT DOME REPOSITORY)

| | Water Level Differences, Meters[*] | |
	1000 Years	10,000 Years
First Estimate	-17	-30
Second Estimate	46	33

[*]Minus sign (-) means water level in the upper aquifer is higher
than in the lower aquifer, implying a downward gradient.

17

Reference

Muller, A. B., N. C. Finley and F. J. Pearson, Jr. Geochemical Parameters Used in the Bedded Salt Reference Repository Risk Assessment Methodology. Sandia National Laboratories. Prepared for the U.S. Nuclear Regulatory Commission. September 1981. SAND-81-0557; NUREG/CR 1996.

3. FUTURE DRILLING

This section adds two comments to the discussion of future drilling scenarios in the Task D Report.

First, the discussion in the Task D Report was not based on a statistical extrapolation from past or present data, but on hypothetical scenarios for future activities at the site. The reason for this approach was the importance of the change in drilling rates with time. Nevertheless, it may be useful in lending perspective to the suggested rate estimates to consider past, present, and estimated future rates on a common scale. Such a comparison is presented in Table 3-1. In comparing U.S. average rates with those for sedimentary rocks, it might be desirable to divide the U.S. average by the fractional area of the sedimentary basins in which most of the drilling has taken place. Using an estimate of 10% for this fraction, this adjustment could raise the rate by one order of magnitude. Similarly, the average rate for basalt and granite would be lowered slightly.

Second, the drilling rates given in the Task D models are based on the assumption of loss of human knowledge and government control of the site after 100 years. This conservative assumption was a guideline for the study. If control of the site is lost but knowledge of the hazard remains, then future drilling scenarios might be somewhat different. Although all discussion of these matters must be speculative, some estimates are appropriate since this is an important concern in siting a repository. The present authors' best estimate is the following: Knowledge of the presence of the repository will do little to deter future drilling, whether or not the government retains control of the site. In fact, if there are signs of potential resources, it is likely that there will be effective pressure to drill for resources on the site even before the hundred-year control period ends. Drillers will pass through the repository level with greater than average care, however, and will monitor for hazardous material. Any associated risk to the drillers becomes their own responsibility, or that of the government

TABLE 3-1

AVERAGE DRILLING RATES: COMPARISON OF PAST, PRESENT, AND
ESTIMATED FUTURE VALUES (HOLES PER SQUARE KILOMETER PER YEAR)

Rock Type	Past Rate, First Estimate[a]	Past Rate, Second Estimate[a]	Past Rate U.S. Average, All Formations[b]	Present Rate, U.S., Average, All Formations[c]	Future Rate, First Estimate[d]	Future Rate, Second Estimate[d]
Bedded Salt	1.3×10^{-4}	2.5×10^{-2}	1.7×10^{-3}	4.0×10^{-3}	2.5×10^{-3}	6.3×10^{-3}
Granite	1.3×10^{-5}	1.3×10^{-4}	1.7×10^{-3}	4.0×10^{-3}	3.1×10^{-4}	2.5×10^{-3}
Basalt	2.1×10^{-4}	5.4×10^{-4}	1.7×10^{-3}	4.0×10^{-3}	1.3×10^{-3}	6.3×10^{-3}
Shale	1.3×10^{-4}	2.5×10^{-2}	1.7×10^{-3}	4.0×10^{-3}	2.5×10^{-3}	6.3×10^{-3}
Dome Salt	8.3×10^{-3}	8.3×10^{-2}	1.7×10^{-3}	4.0×10^{-3}	2.5×10^{-3}	6.3×10^{-3}

(a) Based on existing borehole density, as given in Task D Report, averaged over 30 years. The choice of 30 years is somewhat arbitrary, intended to cover period of heaviest drilling. First and second estimates are as defined in the Task D Report.

(b) Based on 100 years, roughly age of petroleum industry in United States.

(c) Estimated present drilling rate, based on data for recent years.

(d) Based on Task D models, omitting period of above-average drilling rate.

that permits the operation. Some long-term disruption of the repository may also occur through the establishment of an imperfectly sealed borehole pathway, as discussed in the Task D Report. (For example, it may have a hydraulic conductivity of 10^{-4} cm/sec initially or after some degradation.)

4. DEEP DISSOLUTION FEATURES

4.1 INTRODUCTION

Dissolution features have been noted in many salt deposits that are under investigation as potential sites for the disposal of radioactive waste. The possible vulnerability of a repository to dissolution of the protective salt requires careful evaluation of the origin, prevalence, and nature of such features. This section augments the information provided in the Task D Report, and while it does not lead to any revision in the numerical estimates given there, it does highlight the large uncertainties and degree of variability.

"Dissolution feature" describes structures and petrologic changes that result from dissolution of salt and other evaporites, or of less soluble rocks, such as carbonates. In fact, some of these "dissolution features" may not be wholly caused by dissolution, but since dissolution plays an important role in their development, finer distinctions are not useful.

Localized salt dissolution is distinct from regional dissolution, the latter appearing as the progressive and calculable thinning of evaporite deposits at their margins. Localized dissolution is not necessarily accompanied by general salt loss over a large area, but is more erratic, less predictable, and often less easily discerned.

"Deep," as opposed to "shallow" or "surficial," denotes features extending to, or originating near, the bottom of a salt deposit. It is a relative term in that no specific depth is implied.

Although many dissolution features are probably found in most evaporite regions, two types of localized features--breccia pipes and brine pockets-- are of sufficient scale and complexity to be of particular concern for a repository. While there is some controversy over the proper names for these features, "breccia pipe" and "brine reservoir" are used here to denote, respectively, a columnar structure filled with fragmented rock and a void or

permeable zone in a rock formation that yields brine (usually under pressure) when tapped.

4.2 BRECCIA PIPES

Breccia pipes are the more often reported features, since they are often visible at the surface as minor hills or depressions with a core of brecciated rock usually surrounded by upwarped country (surrounding) rock. Whether a hill or depression remains appears to depend upon whether dissolution has lowered the level of the surrounding rock, leaving the insoluble core of the pipe behind. These structures vary somewhat in shape, but most are reported to be roughly circular and from a few meters to hundreds of meters in diameter. In many cases they extend from the bottom of a salt or other soluble stratum to the surface. They are considered collapse structures because the material filling the chimney is brecciated rock typically from overlying formations.

The size of the breccia clasts and their displacement from their original stratigraphic position vary widely, as do their physical properties. Some breccias are reported to be completely cemented with carbonate or evaporite minerals; others are essentially loose and uncemented. It is difficult or impossible to determine the time required for cementation for particular cases.

The processes by which breccia pipes are formed in salt are not completely understood. Three theories are currently prevalent, with all three assuming the existence of some communication between the evaporite deposit and an underlying aquifer. Two theories focus on dissolution and removal of salt to provide void space into which overlying rock may settle. Stanton (1966) hypothesizes that water in contact with salt dissolves and softens the evaporite matrix, permitting the less soluble fractions to detach and float free into what amounts to a slurry of unbound insoluble fragments. He concludes that the void space produced by this process is never very large and that, when overlying rock collapses into the void, the distance of fall is quite small. If the evaporites are under

sufficient stress to flow plastically, evaporite flow would close a cavity as rapidly as it is formed, and brecciation would occur only in overlying strata.

Another theory, based to some extent on laboratory experiments, involves the dissolution of a relatively large cavern through the convective circulation of water under artesian pressure (Anderson, 1978). Under the proper circumstances, fresh (unsaturated) water from a deep aquifer contacts the bottom of a salt deposit through fractures or a permeable zone in an underlying aquiclude. The water becomes saturated with the overlying salt and the dense brine thus formed sinks through the fresh water, bringing more fresh water in contact with the salt. In this way, a convective cell is established and dissolution propagates upward at a rate determined by the relative densities of the fluids. Anderson suggests that a cavity can be formed by this mechanism until it grows too large to support the overburden, whereupon roof-fall occurs and fills the cavity.

The third theory, proposed by Kopf and discussed by Zand (1981), suggests that breccia pipe formation could also result from tectonic and hydrologic interaction. In a manner analogous to the formation of pingos in a permafrost region, Kopf's mechanism involves extreme hydrostatic pressures, induced by tectonism and exceeding the lithostatic stress, that rupture the overburden. Local dissolution could introduce a weak spot and provide an initial pathway for pressurized water to escape. Credence to this theory is supplied by the observations of Christiansen et al. (1981) in their investigation of a blowout structure that penetrates Saskatchewan evaporite deposits and forms Howe Lake. They believe that this structure was formed by the overpressurization of an underlying aquifer during glaciation.

Which mechanism is most instrumental in the formation of a breccia pipe depends largely on local conditions. The first two mechanisms require hydraulic communication between an underlying aquifer and the salt deposit to initiate breccia pipe growth. The third hypothesis does not require communication but does depend upon

the presence of an aquifer below the salt and the (geologically) rapid overpressurization of that aquifer.

4.3 BRECCIA PIPE DISTRIBUTION

Breccia pipes or similar collapse structures have been identified in all of the bedded salt regions under consideration for siting waste repositories, although not all collapse structures have been correlated with deep dissolution. There are, as would be expected, important differences in the location and distribution of breccia pipes among the various salt regions. It is therefore appropriate to discuss each separately.

In the Palo Duro Basin of the Texas Panhandle and neighboring Oklahoma, numerous pipes have been identified and investigated. While there is no complete inventory of these pipes, Gustavson reports at least 78 and alludes to more (Gustavson et al., 1980). In several cases, the pipes are associated with surface drainage. During the construction of Sanford Dam on the Canadian river, 27 pipes were uncovered and more were mapped along the river. Because exposures are best where erosion or regional salt dissolution provide topographic relief, most of the visible pipes have been found along or near valleys or escarpments. It is not yet clear whether pipes are equally distributed throughout the basin, however. The pipes uncovered during construction of Sanford Dam had not been previously recognized; but there has been no similar construction away from the river course that might reveal other undiscovered pipes.

Interpreting the age or rate of development of the Palo Duro features is difficult. Some pipes are overlain with undisturbed Quaternary deposits, while others are filled. In some, the breccia has been cemented with carbonates, but it remains uncemented in others. Since most of the chimneys start in Permian salts and extend through Triassic or younger sediments, it is possible to argue that collapse took place well after deposition. Whether there was a single episode of formation or a steady evolution, or whether

it is continuing today, has not been determined. This is partly due
to the lack of a continuous geologic record for the region. Local
dissolution is largely controlled by the quantity and quality of
water in aquifers underlying the salt deposits. Present conditions
suggest that deep dissolution, if it is taking place, is progressing
at a very slow rate and that there is little evidence for active
dissolution except in association with surface drainage (Stone and
Webster, 1981).

Delaware Basin salt deposits are similarly disrupted by a
number of breccia pipes, although again a complete inventory is not
available. In the immediate (10 km) vicinity of the proposed Waste
Isolation Pilot Plant (WIPP) site, at least four surface features
have been recognized as possible pipes. As in other regions, many
collapse structures may not have reached the surface. Structure
contours of the top of the Salado formation show three times as many
locations where deep dissolution could account for unusual
structures (Sandia, 1978), although there is no evidence to suspect
that all or any are indeed breccia pipes.

Initially, there was thought to be a correlation between the
reef formation encircling WIPP and the dissolution features. More
recent evidence indicates, however, that dissolution is more
scattered across the bottom of the Salado salt deposits (Anderson,
1981 and 1982).

Numerous collapse structures, including breccia pipes, have
been reported in the Paradox Basin (Sugiura & Kitcho, 1981). About
40 structures are mapped in an area of about 52,500 square miles.
Others may exist below the surface. The structures described range
in size from 10 to 150 meters in diameter; breccia within the pipes
may range from well-cemented clasts to uncemented sands and silts.
The age of these collapse structures is difficult to deduce but, as
some are overlain by Quaternary strata, it is likely that they are
as recent as Tertiary, possibly formed contemporaneously with
regional salt anticlines in the Early Tertiary. There also seems to
be a relationship between collapse and faulting, which may be

attributed to groundwater communicating with the salt deposits through faults.

Several locations in the Mackinac Straits region of the Michigan Basin have been identified where breccia structures could be attributed to collapse of overlying rocks into dissolution cavities in salt (Landes, 1945). More locations have been found during recent years. As is the case in most other salt provinces, the numbers of occurrences of pipes cannot be easily established. It is particularly difficult in the Michigan Basin because recent glacial action has obliterated most topographic expressions of breccia pipes, and vegetation and other ground features make exploration difficult.

4.4 BRINE RESERVOIRS

Permeable and porous zones within some deposits may contain trapped water with high concentrations of dissolved material, both solids and gases. These fluid bodies are generally isolated from aquifers and are located in discrete strata or areas within a larger formation. Under certain conditions, brine reservoirs may be economically important and are tapped for their salt content.

While brine reservoirs are distinct to each locale, those found in the Delaware Basin are typical enough to serve as examples. Here, as far as is known, the large reservoirs are essentially restricted to the Anhydrite 2 and Anhydrite 3 zones within the Castile formation (Powers, 1982). Smaller pockets of brine have been found by potash miners drilling into clay seams above the potash ore horizons. The volume of the large reservoirs cannot be determined with accuracy, since few have been tapped and measured, but a number have yielded at least several million gallons of brine. The material contained in these pockets is primarily brine saturated, or nearly saturated, with sodium and calcium salts and showing more than trace quantities of lithium and other cations. Gases—primarily nitrogen, carbon dioxide, and hydrogen sulfide—under high pressure generally accompany these brines.

As previously noted, the reservoirs are generally confined to specific strata. Seismic studies of the Delaware Basin have revealed that the reservoirs are also associated with such structural features as domes, anticlines, and synclines affecting those strata (Powers, 1982). Although not every structure contains a brine reservoir, every known sizable reservoir has been associated with some discernible structure. The extent and height of these structures, together with measured quantities of brine from tapped reservoirs, provide estimates of their area and volume. The only currently available means of confirming that brine is present is to drill into the structure. Since drilling is often difficult or expensive, the extent, nature, and size of brine reservoirs can only be estimated.

4.5 BRINE POCKET DISTRIBUTION

There is less published information for brine pockets than for breccia pipes and similar collapse structures, largely because pockets are usually found through drilling, an expensive and very site-specific technique. Brine reservoirs in the Delaware Basin have already been discussed. In the other regions of interest, brines have occasionally been found, usually during exploration for petroleum or mineral reserves. Except where brines have been of commercial interest, or have ceased to flow soon after discovery, their characteristics have not been well documented.

In the Paradox and Michigan Basins, and around the Salton Sea area, natural brines have been exploited for their mineral content. Most of the brine reservoirs in the Paradox Basin are believed to be small and associated with the evaporites of the Paradox Formation (Stone and Webster, 1981). Michigan Basin brines have been productive for years, but most are apparently the result of dissolution by shallow waters rather than deep dissolution features.

Investigation of the larger brine reservoirs is most active in the immediate vicinity of the WIPP site in the Delaware Basin. Preliminary chemical and radiochronology tests have indicated that

these features are relatively young, with the water on the order of 1 million years old. The water was apparently meteoric, and not the result of dehydration of gypsum or other hydrous minerals (Powers, 1982). Investigations are continuing to determine whether the brine reservoirs represent one stage in the development of breccia pipes, or are independent features. Also remaining to be established is the source of the water in the brine and whether the reservoirs that have been found are still connected to a source. There is some recent evidence that they are actually interconnected and behave like an aquifer (Anderson, 1982).

Earlier studies of brines discovered during potash mining in the Delaware Basin suggest that the recently discovered potash mine brines are decidedly different (GEI,1978). A survey of six mining operations revealed that the brine pockets encountered were generally confined to clay strata near the ore horizons. The volume of brine usually was no more than 10,000 gallons, seldom required pumping, and was never sufficient to disrupt mining operations.

4.6 DETECTION METHODS

Locating deep dissolution features by existing techniques requires both luck and judgment. Standard methods for finding collapse features usually include topographic examination, assisted by aerial or satellite photography and field checking. If the surface expression of a feature warrants further study, seismic surveys may be performed to determine if the underground form of the structure is consistent with breccia pipes. Finally, drilling is necessary to confirm the nature of a structure. Similarly, brine reservoirs may be found through a combined field and seismic survey. Confirmation of the existence of deep brine also depends upon drilling into the structure.

Neither drilling nor seismic surveying can be accomplished quickly or inexpensively, and most investigators believe that many buried features remain undiscovered. Furthermore, an extensive drilling program around a potential repository site may do more to

compromise the integrity of the site than the mere presence of a pipe or brine reservoir.

References

Anderson, R. Y. Deep Dissolution of Salt, Northern Delaware Basin, New Mexico. Report to Sandia Laboratories. 1978.

_____ Deep-seated Salt Dissolution in the Delaware Basin, Texas and New Mexico. New Mexico Geological Society Special Publication No. 10, 133-145. 1981.

_____ Upper Castile Brine Aquifer Northern Delaware Basin New Mexico. Department of Geology, University of New Mexico. April 1982.

Christiansen, E. A., D. J. Gendzwill, and W. A. Meneley. Howe Lake: A Hydrodynamic Blowout Structure. Preprint, 1981.

Geotechnical Engineers, Inc. (GEI). Final Report on Uncertainties in the Detection, Measurement, and Analysis of Selected Features Pertinent to Deep Geologic Repositories. July 10, 1978.

Gustavson, T. C. et al. The University of Texas at Austin. Geology and Geohydrology of the Palo Duro Basin, Texas Panhandle. Prepared for the U.S. Department of Energy. 1980.

Landes, K. K. Mackinac Breccia, Chap. 3 p. 121-154. In: Geology of the Mackinac Straits Region and Sub-surface Geology of Northern Southern Peninsula. (Landes, K. K., G. M. Ehlers and G. M. Stanley, eds.). Mich. Geological Society Pub. 44, Geol. Ser. 37, 204 p., 1945.

Powers, D. W., Sandia National Laboratory, personal communication, 1982.

Sandia Laboratories (Powers, D. W. et al., eds.). Geological Characterization Report, Waste Isolation Pilot Plant (WIPP) Site, Southeastern New Mexico. Prepared for the U.S. Department of Energy. August 1978. SAND 78-1596.

Stanton, R. J., Jr. The Solution Brecciation Process. Geological Society of America Bulletin, No. 77, pp. 843-848, August 1966.

Stone & Webster Engineering Corporation. Area Geological Characterization Report for the Palo Duro and Dalhart Basins, Texas. Prepared for the Office of Nuclear Waste Isolation. December 1981. ONWI-292.

Sugiura, R. and C. A. Kitcho. Collapse Structures in the Paradox Basin. Rocky Mountain Association of Geologists—1981 Field Conference.

Zand, S. M. State of New Mexico, Environmental Evaluation Group. Dissolution of Evaporites and Its Possible Impact on the Integrity of the Waste Isolation Pilot Plant (WIPP) Repository. September 15, 1981. EEG-14.

5. SOLUTION MINING

5.1 INTRODUCTION

Solution mining was not modeled as a separate failure element in the Task D Report. The decision not to do so was based on the belief that a repository would be detected during the preliminary drilling and testing associated with the development of a solution mine. Furthermore, since salt deposits are widespread and solution mining is limited, even the consideration of solution mining at a repository site was regarded as a highly improbable event. This section reexamines this approach on the basis of a more extensive review of available information, including the more recent salt dome siting studies.

5.2 BEDDED SALT

There are approximately 30 salt solution mines in bedded salt regions of the United States, with at least one such operation in each of the Permian, Paradox, Silurian, and Williston Basins (USGS, 1970; United States Department of Interior, 1980). (Another 15 or so solution mines in the salt domes of the Gulf Region are discussed in Section 5.3.) All the mines are mining sodium chloride except for one potash solution mine in the Paradox Basin; a solution mine for trona (a sodium mineral) is being developed in Wyoming. Adding the number of solution cavities developed for other purposes, such as underground storage, in the same regions, it appears that there are 50 to 100 such operations in the United States. On the other hand, there are about 1 million drillholes in those regions to a depth that may be considered relevant to a repository (Task D Report). Thus, if the repository site becomes available for exploration or exploitation, and if drilling and solution mining continue in the future at a ratio similar to that of the past, drilling would probably lead to discovery of the repository before solution mining.

5.3 DOME SALT

The situation with salt dome deposits is quite different from that with bedded salt. Whereas there may be only about 50 solution mining operations in 8×10^5 km^2 of evaporite basins in the United States, there may be an equal number within the approximately 250 salt domes in the Gulf Region. Given the relatively small size of most salt domes (a few square kilometers), this number represents much greater exploitation of the available resource. Furthermore, dome salt has certain properties that make it a favorable target for solutioning. These properties include generally higher purity, lower likelihood of continuous interbeds and other structures that can cause leaks from storage cavities, and much greater thickness. As pointed out in the Task D Report, there are multiple, often competing, uses for salt domes, as illustrated in Figure 5-1. The geometry of past solutioning cavities in one salt dome is shown in Figure 5-2, taken from an environmental impact study for its use as part of the Strategic Petroleum Reserve (Federal Energy Administration, 1976). Numerical data characterizing the cavities shown in Figure 5-2 are given in Table 5-1.

The U.S. Department of Energy and its contractors have recently carried out studies to identify salt domes with potential for a nuclear waste repository. For several reasons, such as greater salt dome stability and distance from the sea, the effort focused on the salt domes of the Gulf Interior region. Seventeen criteria and screening specifications were used, but three of the criteria dominated the screening (Law Engineering, 1980).

1) Dome tops should be at depths less than about 3000 feet.

2) Domes should have areas greater than 1000 acres in lateral extent, plus a 500-foot buffer zone.

3) Domes should not have been used by industry for production, storage, or other mineral-related use.

36

RADIOACTIVE WASTE ISOLATION
UNDERGROUND DEGRADATION OF WASTE
SOLUTION MINE
DRY SALT MINE
SPACE FOR UNDERGROUND STRUCTURES
CHEMICAL REACTION CHAMBER
AIR STORAGE FOR PEAKING POWER
HYDROCARBON STORAGE
OIL AND GAS DEVELOPMENT
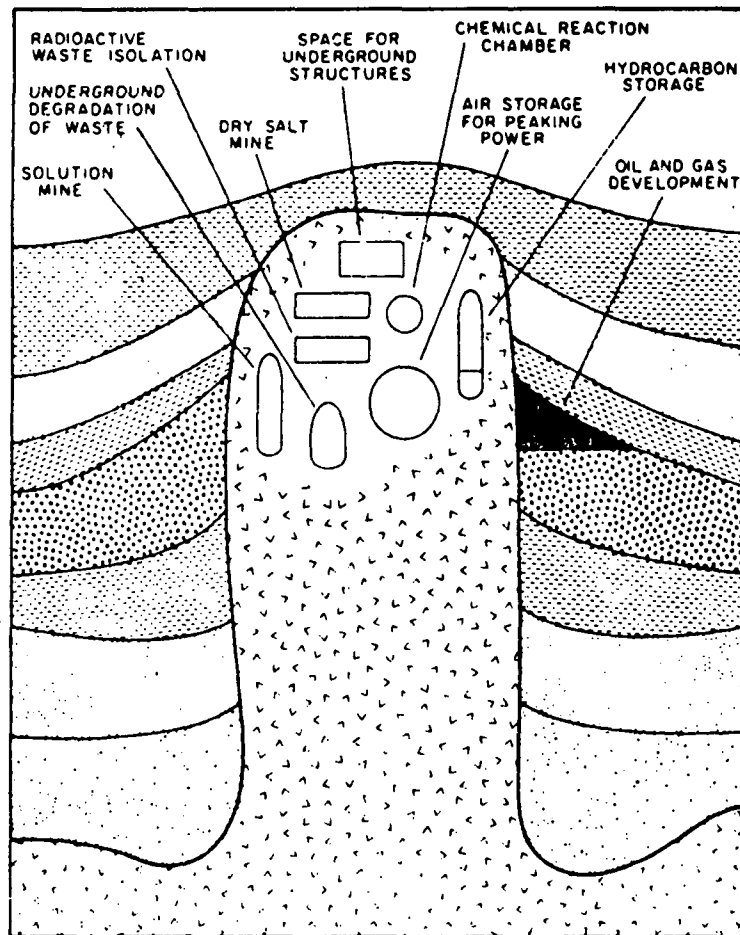
Source: Martinez and Thoms, 1978.

FIGURE 5-1   POTENTIAL DEMANDS FOR SALT DOME UTILIZATION

37
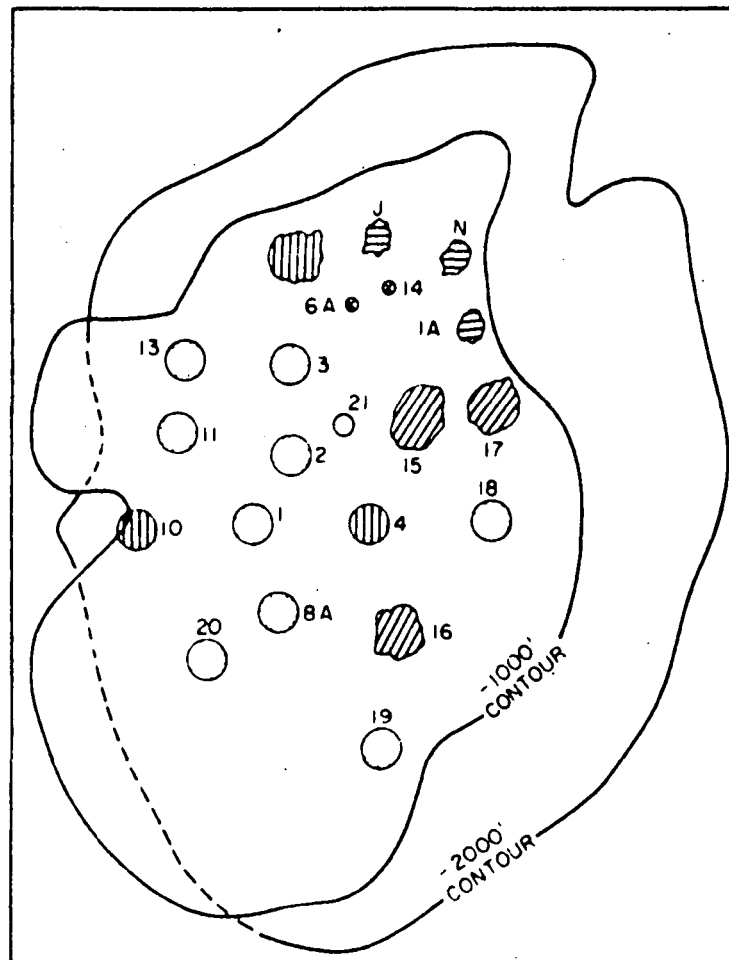
LEGEND

⊕ ABANDONED – NOT USABLE
⊖ COMMITTED STORAGE
◯ USABLE CAVERNS
⊛ UNDEVELOPED CAVERNS
⊘ COMMITTED AVAILABLE STORAGE SPACE

```
0        500   1000              2000
|━━━━━━━━━━━━━━━|━━━━━━━━━━━━━━━━━|
              FEET
```

Source: Martinez and Thoms, 1978. Modified from Federal
           Energy Administration, 1976.

FIGURE 5-2   CAVITY DEVELOPMENT IN A GULF COAST SALT DOME

38

TABLE 5-1

DATA ON CAVITIES SHOWN IN FIGURE 5-2

Cavity	Top of Cavity (depth/ft)	Bottom of Cavity (depth/ft)	Maximum Diameter/ Height (ft)	Gross Volume x 10^3 (ft^3)
1	988	1816	418/1007	8,102
2	741	1608	*/1121	6,000
3	876	1830	295/1130	4,236
8A	1242	1978	235/765	3,155
11	1067	1812	400/953	10,454
13	1112	1883	300/918	5,055
15	2597	3297	480/980	16,618
16	2620	3264	*/644	8,800
17	2598	4043	295/1543	12,175
18	3500	4285	480/883	10,000
19	2980	4312	415/1420	9,000
20	4126	4328	355/326	6,000
21	New Solution Well			

*No sonar caliper survey available

Source: Martinez and Thoms, 1978.

Most domes failed to meet one or more of these criteria, as shown in Table 5-2, which indicates some of the reasons for failure. Eleven domes were identified; the number was later reduced to seven. These seven domes were then studied in greater detail. Among the results were a set of rankings on the basis of resource value for mineral development or other purposes, as shown in Table 5-3 (Law Engineering, 1980). The potential for the production of brine or salt is very high, as is the potential for use for various types of underground storage. The cited study points out that there are many other domes with equally favorable characteristics for brining or salt mining, and the use of one of these domes would not represent the loss of a unique resource. Nevertheless, given the basic assumptions of this study (Task D Report, p. 208), it cannot be assumed that knowledge of the existence of the repository or control of the site will deter site use after 100 years. It appears obvious, therefore, that under these assumptions there is a very high probability that solution mining, for any of several purposes, will take place in the future. Furthermore, it is quite possible that the repository would go unnoticed during part or all of this operation.

This conclusion arises from the premises for the Task D study. Stated differently, it does not say that solution mining will probably occur in a salt dome repository, but only that prevention of such mining is dependent on human controls indefinitely into the future.

TABLE 5-2

RESULTS OF REGIONAL CHARACTERIZATION SCREENING

NORTHEAST AND SOUTH TEXAS BASINS

Dome	Recommended	Reason for Tentative Elimination
Bullard	no	Less than 1000 acres 500' barrier
PALESTINE	yes	-
Brooks	no	Lake
Grand Saline	no	Brine production
Steen	no	Less than 1000 acres +500' barrier
Butler	no	LPG storage, too small
Whitehouse	no	Less than 1000 acres +500' barrier
KEECHI	yes	-
Palangana	no	Brine and sulfur prod.
Mt. Sylvan	no	Urban and airport
Gyp Hill	no	Less than 1000 acres +500' barrier
East Tyler	no	LPG storage
OAKWOOD	yes	-
Hainesville	no	LPG storage
Piedras Pintas	no	Petroleum production
Bethel	no	Less than 1000 acres +500' barrier
Boggy Creek	no	Under major river
Day	no	More than 915 m deep
Brushy Creek	no	More than 915 m deep
Kittrell	no	More than 915 m deep
La Rue	no	More than 915 m deep
Concord	no	Less than 1000 acres +500' barrier & more than 915 m deep
Moca	no	More than 915 m deep
Dilworth Ranch	no	More than 915 m deep
Pescadito	no	More than 915 m deep

NORTH LOUISIANA BASIN

Dome	Recommended	Reason for Tentative Elimination
RAYBURNS	yes	-
Kings	no	Less than 1000 acres +500' barrier
Winnfield	no	Less than 1000 acres +500' barrier
Cedar Creek	no	Less than 1000 acres +500' barrier
VACHERIE	yes	-
Drakes	no	Less than 1000 acres +500' barrier
Gibsland	no	LPG storage
Protho	no	Petroleum production & too small
Prices	no	Less than 1000 acres +500' barrier
Arcadia	no	LPG storage
Minden	no	Petroleum production
Bistineau	no	Less than 1000 acres +500' barrier
Coochie Brake	no	Economic-held in reserve
Chestnut	no	Less than 1000 acres +500' barrier
Milam	no	Less than 1000 acres +500' barrier & more than 915 m deep
Chester	no	Less than 1000 acres +500' barrier & more than 915 m deep
Sikes	no	Less than 1000 acres +500' barrier & more than 915 m deep
Packton	no	Less than 1000 acres +500' barrier & more than 915 m deep
Castor Creek	no	Less than 1000 acres +500' barrier

MISSISSIPPI BASIN

Dome	Recommended	Reason for Tentative Elimination
McIntosh	no	Brine production
RICHTON	yes	-
Crowville	no	Less than 1000 acres +500' barrier
Tatum	no	Less than 1000 acres +500' barrier & nuclear test site
LAMPTON	yes	-
Petal	no	LPG storage
Gilbert	no	Less than 1000 acres +500' barrier
Hazelhurst	no	Less than 1000 acres +500' barrier
Arm	no	Less than 1000 acres +500' barrier
McLaurin	no	Less than 1000 acres +500' barrier
Richmond	no	Less than 1000 acres +500' barrier
Bruinsburg	no	Less than 1000 acres +500' barrier
Byrd	no	Less than 1000 acres +500' barrier
Leedo	no	Less than 1000 acres +500' barrier
Raleigh	no	Less than 1000 acres +500' barrier

MISSISSIPPI BASIN (Continued)

Dome	Recommended	Reason for Tentative Elimination
McBride	no	Less than 1000 acres +500' barrier
County Line	no	Less than 1000 acres +500' barrier
Moselle	no	Less than 1000 acres +500' barrier
Sardis Church	no	Less than 1000 acres +500' barrier
Dont	no	Less than 1000 acres +500' barrier & 66 Dry Creek no Less than 1000 acres +500' barrier
Centerville	no	Less than 1000 acres +500' barrier
D'Lo	no	Less than 1000 acres +500' barrier
Eminence	no	Less than 1000 acres +500' barrier
Midway	no	Less than 1000 acres +500' barrier
New Home	no	Less than 1000 acres +500' barrier
Oakley	no	Less than 1000 acres +500' barrier
Oakvale	no	Less than 1000 acres +500' barrier
Ruth	no	Less than 1000 acres +500' barrier
Walnut Bayou	no	Less than 1000 acres +500' barrier
Monticello	no	Less than 1000 acres +500' barrier
Allen	no	Less than 1000 acres +500' barrier
Prentiss	no	Less than 1000 acres +500' barrier
Carmichael	no	Less than 1000 acres +500' barrier & more than 915 m deep
Bothwell	no	Less than 1000 acres +500' barrier & more than 915 m deep
South Tallulah	no	More than 915 m deep
Edwards	no	More than 915 m deep
Caseyville	no	More than 915 m deep
Kola	no	More than 915 m deep
Carson	no	More than 915 m deep
Utica	no	More than 915 m deep
Coleman	no	More than 915 m deep
Hervey	no	More than 915 m deep
Wesson	no	More than 915 m deep
Kings	no	More than 915 m deep
Halifax	no	More than 915 m deep
Glass	no	More than 915 m deep
Ashwood (Somerset)	no	More than 915 m deep
Newellton	no	More than 915 m deep
Singer	no	More than 915 m deep
Vicksburg	no	More than 915 m deep
Eagle Bend	no	More than 915 m deep
Galloway	no	More than 915 m deep
Learned	no	More than 915 m deep
North Tallulah	no	More than 915 m deep
Brownsville	no	More than 915 m deep
Oakridge	no	More than 915 m deep
Newman	no	More than 915 m deep
Duck Port	no	More than 915 m deep
Sunrise	no	More than 915 m deep
Snake Bayou	no	More than 915 m deep
Foules	no	More than 915 m deep
Glazier	no	More than 915 m deep
Heidleberg	no	More than 915 m deep
Gwinville	no	More than 915 m deep
South Carolton	no	More than 915 m deep
Burns	no	More than 915 m deep
Yellow Creek	no	More than 915 m deep
Eucutta	no	More than 915 m deep
Laurel	no	More than 915 m deep
Valley Park	no	More than 915 m deep
Rufus	no	More than 915 m deep
Ovette	no	More than 915 m deep
Hiwanee	no	More than 915 m deep
Baxterville	no	More than 915 m deep
Ellisville	no	More than 915 m deep
Grange	no	More than 915 m deep
CYPRESS CREEK (New Augusta)	yes	-
Hubbard	no	Less than 1000 acres +500' barrier & more than 915 m deep
Zion Hill Church	no	Less than 1000 acres +500' barrier

41

Source: Law Engineering Testing Company, 1980

TABLE 5-3

RESOURCE VALUES OF POTENTIALLY SUITABLE SALT DOMES

POTENTIAL RESOURCE OR USE	KEECHI	OAKWOOD	RAYBURNS	VACHERIE	CYPRESS CREEK	LAMPTON	RICHTON
--------Potential Rank on Scale of 1-10 (Highest)---------							
ABSORBENT MINERALS	0-1	0-1	0-1	0-1	0-1	0-1	0-1
AGRICULTURAL LIME	1-<1	0-<1	1	0-<1	0-<1	0-<1	0-<1
AGRICULTURAL PRODUCTS AND FARMING	3-6	3-6	3-7	3-7	3-7	3-7	3-7
AMBER	0	0	0	0	0	0	0
ASPHALTIC ROCK	3-4	0-<1	0-<1	0-<1	0-<1	0-<1	0-<1
BAUXITE AND BAUXITIC CLAY	<1	<1	<1	<1	0-<1	0-<1	0-<1
BENTONITE AND OTHER VOLCANIC MATERIALS	1-2	1-2	1-2	1-2	1	1	1
BITTERNS	0-<1	0-<1	0-<1	0-<1	0-<1	0-<1	0-<1
BLEACHING CLAYS	0-1	0-1	0-1	0-1	0-1	0-1	0-1
BRINES	9-10	8-10	9-10	8-10	7-10	6-10	8-10
BUILDING STONE	0-<1	0-<1	0-<1	0-<1	0-<1	0-<1	0-<1
CARBON DIOXIDE	1-2	1-2	1-2	1-2	1-3	1-3	1-3
CEMENT MATERIALS	1-2	0-1	1-2	0-1	0-1	0-1	0-1
CLAYS AND CLAY MATERIALS	1	1	1	1	1	1	1
CHALK, MARL & LIMESTONE	1-2	0-1	1-2	0-1	0	0	0
CHERT & TRIPOLI	0	0	0	0	0	0	0
COAL (SEE LIGNITE)	0	0	0	0	0	0	0
CONSTRUCTION MATERIAL	1-3	1-3	1-3	1-3	1-3	1-3	1-3
FOUNDRY SAND	0	0	0	0	0	0	0

TABLE 5-3 (continued)

POTENTIAL RESOURCE OR USE	KEECHI	OAKWOOD	RAYBURNS	VACHERIE	CYPRESS CREEK	LAMPTON	RICHTON
FULLER'S EARTH	0	0	0	0	0	0	0
GEOTHERMAL & GEOPRESSURED MATERIALS	3-4	3-4	3-4	3-4	3-4	3-4	3-4
GLASS SAND	1-2	1-2	1-2	1-2	1-2	1-2	1-2
GLAUCONITE	1-2	1-2	1-2	1-2	0-1	0-1	0-1
GYPSUM	0-<1	0-<1	0-<1	0-<1	0-<1	0-<1	0-<1
HEAVY MINERALS	±1	±1	±3	±3	±3	±3	±3
HYDROGEN SULFIDE	±1	±1	±1	±1	3-4	3-4	3-4
IRON ORE	<1	<1	1-2	1-2	0-<1	0-<1	0-<1
KAOLIN & KAOLINITIC CLAY	1	1	<1	<1	0	0	0
LIGHTWEIGHT AGGREGATE	±1	±1	±1	±1	±1	±1	±1
LIGNITE	4-6	4-6	3	4-6	0-<1	1-2	0-<1
MANGANESE	0	0	0	0	0	0	0
MEDICINE SALTS	0-<1	0-<1	0-<1	0-<1	0-<1	0-<1	0-<1
MINERAL FILLERS	±1	±1	±1	±1	±1	±1	±1
OIL AND NATURAL GAS	1-2	2+	±1	1-2	2+	±1	±1
PEAT	0	0	0	0	0-1	0	0
PIGMENTING MATERIALS AND OCHRE	±1	±1	±1	±1	±1	±1	±1
POZZOLANIC MATERIALS	>1	>1	>1	>1	>1	>1	>1
RECREATION & GENERAL USE	5-10	5-10	5-10	5-10	5-10	5-10	5-10
REFRACTORY MATERIALS	±1	±1	±1	±1	±1	±1	±1
ROAD MATERIALS	1-4	3-4	1-4	3-4	3-4	3-4	3-4
ROCK PHOSPHATES	0-<1	0-<1	0-<1	0-<1	0-<1	0-<1	0-<1

TABLE 5-3 (continued)

POTENTIAL RESOURCE OR USE	KEFCHI	OAKWOOD	RAYBURNS	VACHERIE	CYPRESS CREEK	LAMPTON	RICHTON
SALTS	9-10	9-10	9-10	8-10	8-10	8-10	8-10
SAND & GRAVEL	2-3	3-4	2-3	3-4	3-4	3-4	3-4
SHELLS	0	0	0	0	0	0	0
SULFUR	0-1	0-1	0-1	0-1	0-1	0-1	0-1
UNDERGROUND STORAGE	7-9	7-9	7-9	7-9	7-9	7-9	7-9
USUAL GASES (SEE CO_2 & H_2S)	0-<1	0-<1	0-<1	0-<1	0-<1	0-<1	0-<1
URANIUM	<1	<1	<1	<1	<1	<1	<1

*Best-guess estimate rankings of potential mineral resources and uses, based on available data and subject to modification with changes in data or knowledge.

1	Non-prospective, non-exploitable, or non-usable
0-1	Negligible to speculative
1-3	Poor to fair
4-6	Fair to good
7-9	Good to excellent
10	Productive/in use or capable of production/use

Source: Law Engineering Testing Company, 1980.

References

Federal Energy Administration. Strategic Petroleum Reserve - Final Environmental Impact Statement for Bayou Choctaw Salt Dome. 1976. FES 76-5; FEA/S-76/501.

Law Engineering Testing Company. Geologic Area Characterization. Volume 1: Introduction, Background, and Summary. Gulf Coast Salt Domes Project. Prepared for Battelle Memorial Institute. August 29, 1980.

Martinez, J. D. and R. L. Thoms. A Systems Concept of Space Utilization in Gulf Coast Salt Domes. In: Storage in Excavated Rock Caverns. (Magnus Berman, ed.), Rochester 77, 1. Pergamon Press, New York, 1978.

U.S. Department of the Interior, Geological Survey (USGS). The National Atlas of the U.S.A. 1970.

U.S. Department of the Interior, Bureau of Mines. Mineral Facts and Problems. 1980.

6. THERMAL BUOYANCY MODEL

The Task D Report describes a simplified method of analyzing the effect of heat generated by radioactive wastes on vertical groundwater flow (Appendix D-VI). This method requires the following data:

- Temperature distribution in the overlying rock at the time of interest.

- Water density as a function of temperature.

- Water viscosity as a function of temperature.

- Hydraulic conductivity of the water column pathway.

- Effective porosity of the water column pathway.

This information is entered into the computational framework illustrated in Figure 6-1. The output from the computations are volumetric flow rates and travel times for water from the repository to an overlying aquifer when driven by the thermally induced buoyancy effect.

To evaluate the reasonableness of this approach, the simplified model was applied to the generic granite repository described in Dames & Moore (1978). Comparison of the results of the Task D approach with those of detailed numerical simulations gives further evidence that application of the simplified model is adequate for generic repository evaluations. Figure 6-2, which is taken from the Dames & Moore report, is a schematic of the reference granite repository. The repository is located at a depth of 2000 feet (610 meters) below the land surface in unweathered granite. The granite stratigraphic section was described as having four zones with different hydraulic characteristics, as shown in Table 6-1.

```
┌─────────────────────────┐
│ S1                      │
│   Pick time t.          │
└─────────────────────────┘
            │
┌─────────────────────────┐
│ S2                      │
│   Obtain temperature    │
│   distribution from     │
│   other documents.      │
└─────────────────────────┘
            │
┌─────────────────────────┐
│ S3                      │
│   Compute corresponding │
│   density distribution. │
└─────────────────────────┘
            │
┌─────────────────────────┐         ┌──────────────────────────┐
│ S4                      │         │ S5                       │
│   Compute mass of       │         │   Compute mass of column │
│   vertical column       │         │   of water at normal tem-│
│   of water.             │         │   perature.              │
└─────────────────────────┘         └──────────────────────────┘
            │
┌─────────────────────────┐
│ S6                      │
│   Determine vertical    │
│   force on column and   │
│   corresponding pressure.│
└─────────────────────────┘
            │
┌─────────────────────────┐         ┌──────────────────────────┐
│ S7                      │         │ S8                       │
│   Convert to equivalent │         │   Compute water          │
│   hydraulic gradient.   │         │   viscosity for ambient  │
│                         │         │   conditions.            │
└─────────────────────────┘         └──────────────────────────┘
            │
┌─────────────────────────┐
│ S9                      │
│   Determine flow rates  │
│   and interstitial      │
│   velocity by Darcy's   │
│   law.                  │
└─────────────────────────┘
            │
┌─────────────────────────┐
│ S10                     │
│   Determine travel time │
│   from repository to    │
│   aquifer.              │
└─────────────────────────┘
```

Source: Task D Report.

FIGURE 6-1   INFORMATION FLOW CHART FOR BUOYANCY COMPUTATIONS

Low Ground Relief

Water Table Slope = Regional Dip

Ground Surface

Depth (ft)
0

Weathered Granite $K_x = K_y = 5 \times 10^{-4}$ cm/s

Partially Weathered Granite $K_x = K_y = 5 \times 10^{-6}$ cm/s

Repository
2000 ft depth

Unweathered Granite $K_x = K_y = 5 \times 10^{-8}$ cm/s

$K_x = K_y = 5 \times 10^{-9}$ cm/s

Lower Boundary (considered impermeable)

Recharge Boundary

Discharge Boundary

Distance in thousands of feet
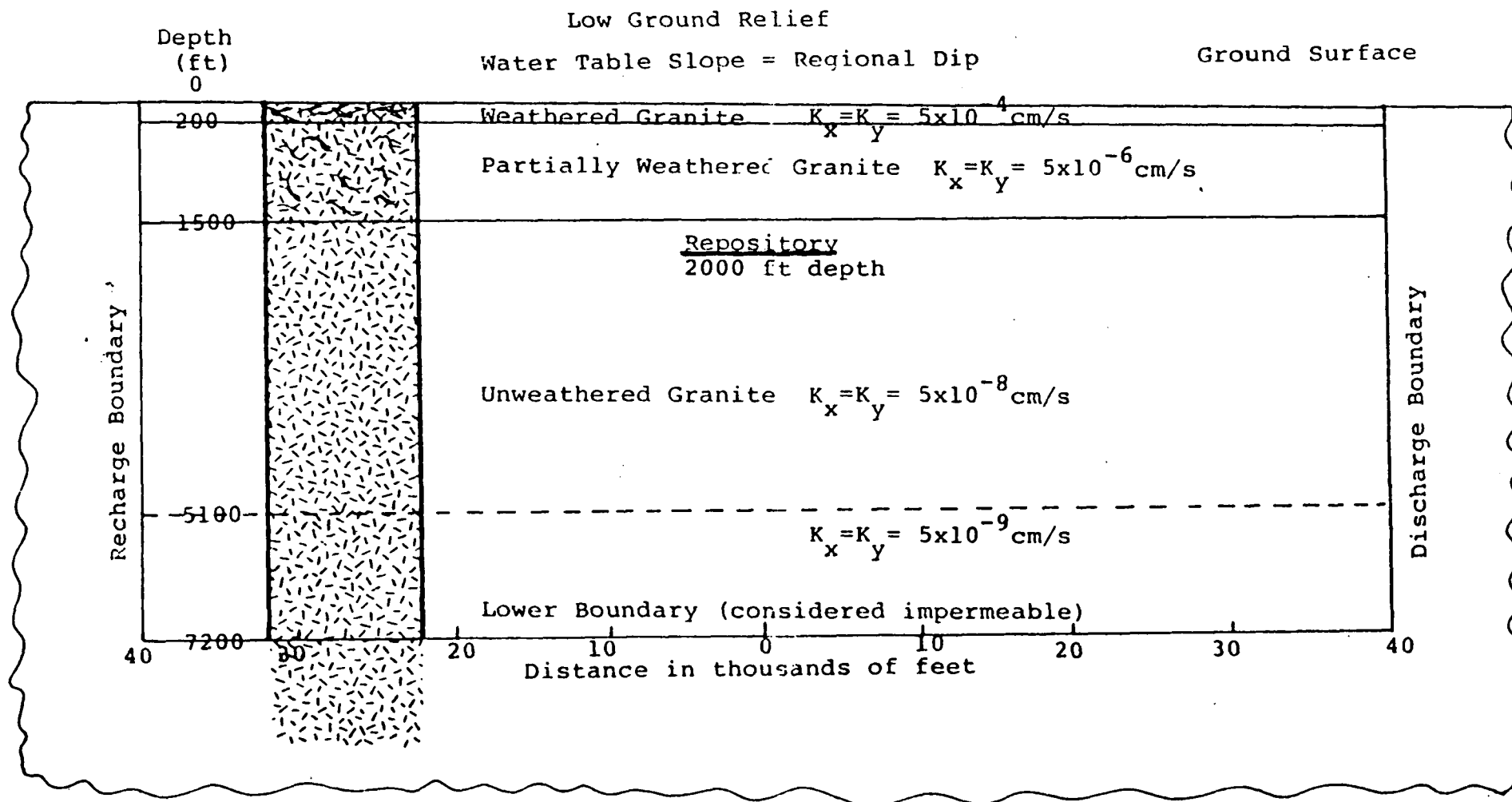
Source: Dames & Moore, 1978.

FIGURE 6-2   GENERIC GRANITE STRATIGRAPHIC SECTION IN ITS REGIONAL SETTING

TABLE 6-1

HYDRAULIC CHARACTERISTICS OF THE GENERIC
GRANITE STRATIGRAPHIC SECTION

Depth, Meters (ft)	Isotropic Hydraulic Conductivity	Effective Porosity	cm/s
0-61 (0-200)	5×10^{-4}	1×10^{-3}	10^{-3}
61-457 (200-1500)	5×10^{-6}	1×10^{-4}	10^{-4}
457-1554 (1500-5100)	5×10^{-8}	1×10^{-4}	10^{-4}
1554-2195 (5100-7200)	5×10^{-9}	1×10^{-4}	10^{-4}

Note: For flow calculations, the three zones that extend from the land surface to the repository depth (610 meters) can be represented by an equivalent zone 156 meters thick with a vertical hydraulic conductivity of 5×10^{-8} cm/s.

Source: Dames & Moore, 1978.

The Task D model uses the following equation to calculate travel time from the repository to the overlying aquifer:

$$\tau = \frac{D}{\left(\dfrac{Ki}{100\mu\eta}\right)} \qquad (6.1)$$

where

τ = travel time from the repository to the overlying

    aquifer or target horizon, years.

D = distance from the repository to the overlying

    aquifer or target horizon, meters.

K = hydraulic conductivity, meters/year.

i = effective thermal buoyancy gradient, dimensionless.

$100~\mu$ = viscosity of water at the representative temperature

    divided by the viscosity of water at 20°C, dimensionless.

η = effective porosity, dimensionless.

The viscosity term is based on the average temperature of the water column and the gradient term is related to the average density of the water column by:

$$i = 1 - \rho^* \qquad (6.2)$$

when ρ^* is the average density of the water column under consideration.

To estimate the appropriate viscosity and gradient terms, a running profile of water density is plotted from the overlying aquifer to below the repository and the representative water density is determined when the incremental density addition equals (approximately) the average density of the column. (Cf. Appendix D-VI.) The gradient term is calculated by Eq. (6.2), and the viscosity term is based on the average water temperature as estimated from the average water density. Substituting values used

for the representative generic granite section (D = 156 meters, K = 1.58 x 10^{-2} meters/year, η = 10^{-4}) into Eq. (6.1) yields

$$\tau = 100 \left(\frac{\mu}{i}\right) \text{ years.}$$

Following the method described in the Task D Report, the estimated travel time for the generic granite repository 1000 years after repository sealing is determined by plotting temperature profiles from the calculated temperature distribution data included in the Dames & Moore report. There is one profile for a 100 kW/acre loading rate and another for a 200 kW/acre loading rate, included as Figures 6-3 and 6-4. These profiles are also indicative of density variations. From Figure 6-3 the average density of the water column with maximum vertical velocity may be estimated to correspond to an average temperature of 30 - 50°C. Similarly, from Figure 6-4 an average temperature of 40 - 60°C may be estimated. Table 6-2 contains the viscosity, density, gradient, and travel times corresponding to these temperature values.

Table 6-2 shows that using the Task D model, calculated travel time from the repository to land surface for the generic granite repository with a 100 kW/acre loading rate is between 45 and 205 years, compared with 100 years using the numerical model (Dames & Moore, 1978, Table 2-3). For a 200 kW/acre loading rate, the calculated travel time with the simplified model is between 30 and 80 years, compared with 40 years using the numerical model (Dames & Moore, 1978, Table 2-3). The close agreement between the calculated travel times of the simplified model and the numerical model suggests that for generic repository analyses the simplified model is adequate.

Using an effective porosity (η) of 10^{-4} for the whole section instead of making an adjustment for the higher effective porosity (10^{-3}) reported for the weathered granite reduces the calculated travel time by less than one year.

52
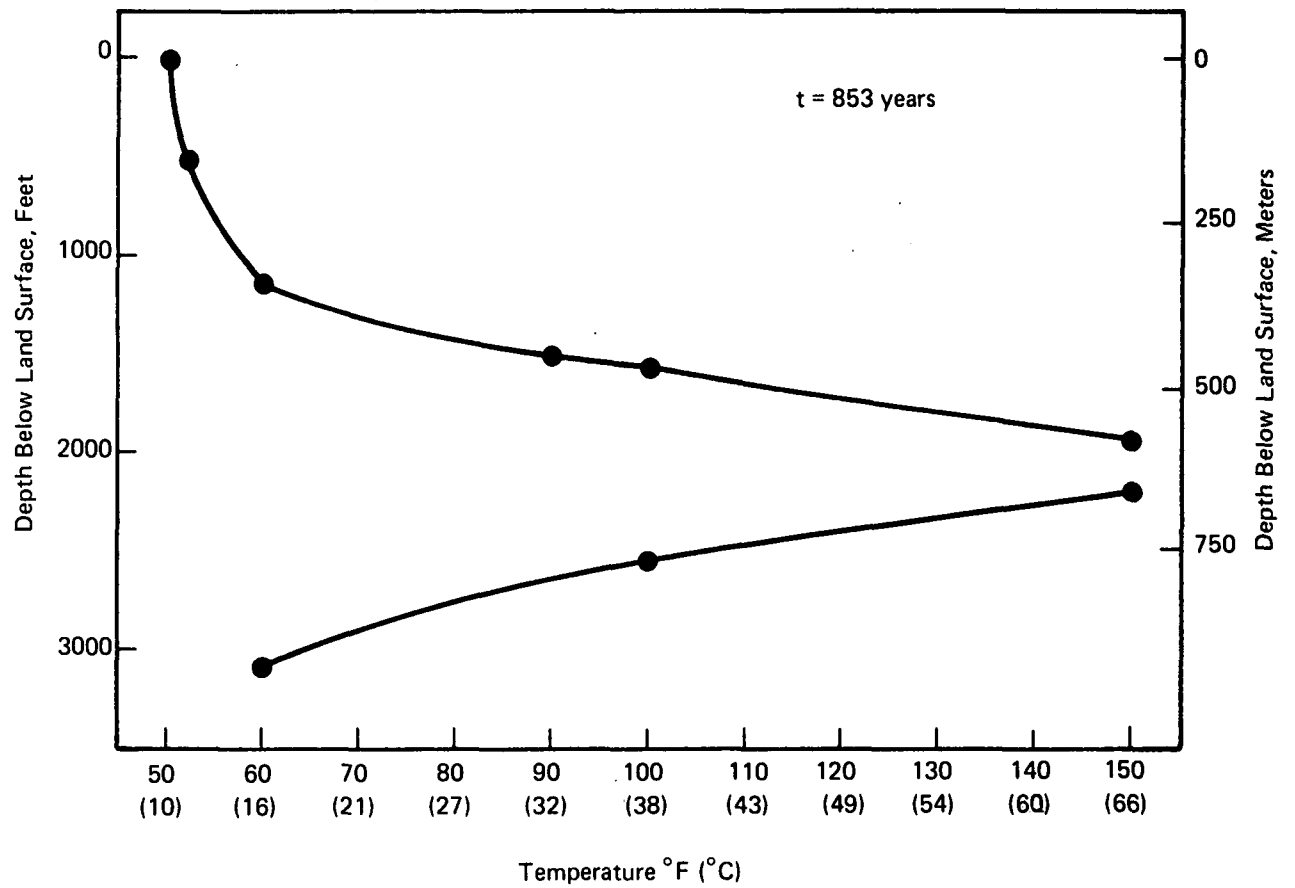
Source: Adapted from Dames & Moore, 1978.

FIGURE 6-3   TEMPERATURE DISTRIBUTION PROFILE FOR GENERIC GRANITE REPOSITORY AT A THERMAL LOADING RATE OF 100 KW/ACRE
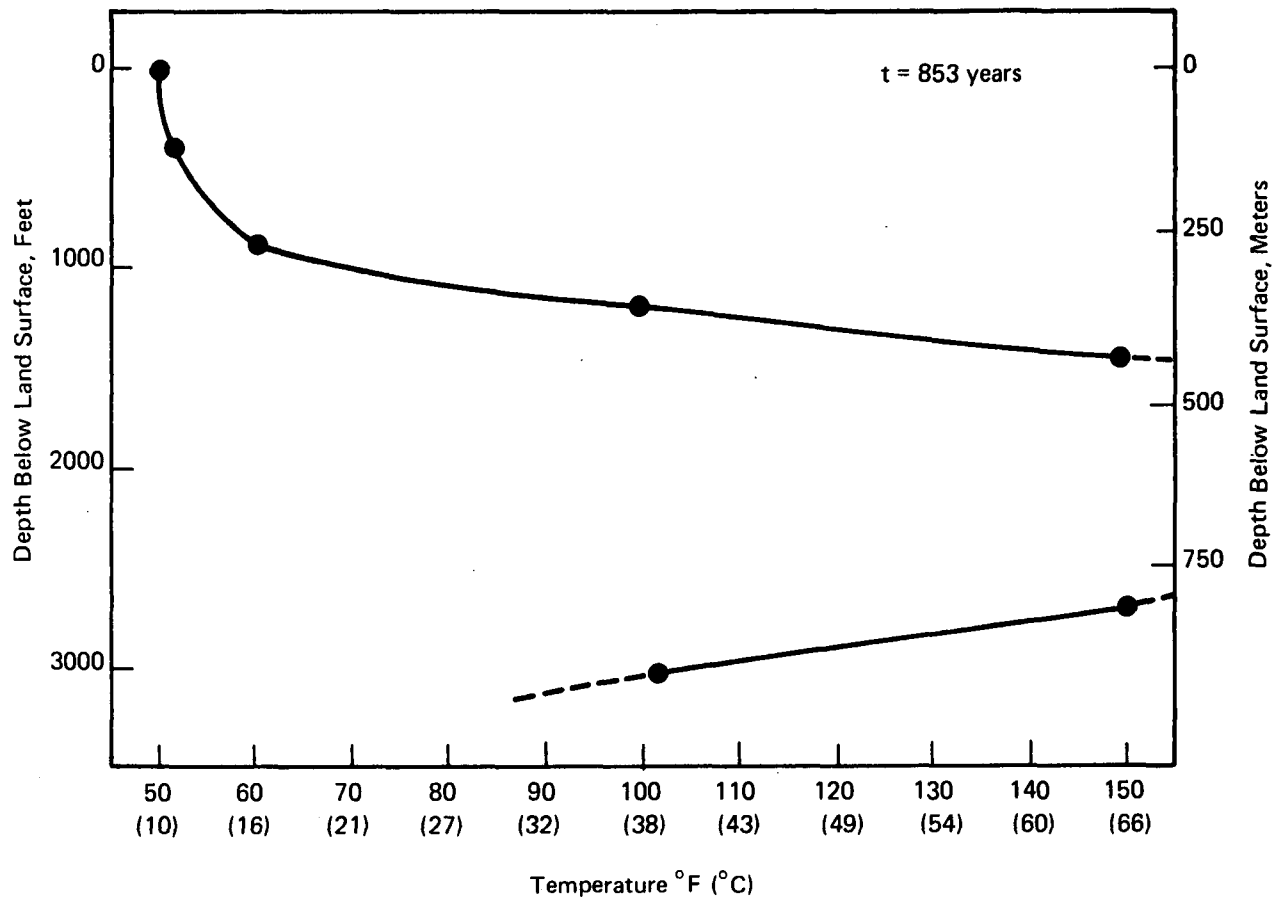
Source: Adapted from Dames & Moore, 1978.

FIGURE 6-4   TEMPERATURE DISTRIBUTION PROFILE FOR GENERIC GRANITE
REPOSITORY WITH A THERMAL LOADING RATE OF 200 KW/ACRE

TABLE 6-2

WATER VISCOSITY, DENSITY, HYDRAULIC GRADIENT AND
MINIMUM TRAVEL TIME FOR SELECTED REPRESENTATIVE TEMPERATURES

Temperature °C	Viscosity, μ, Poise	Density, ρ* gm/cm^3	Gradient, i	Time, τ years
30	.0082	.996	.004	205
40	.0065	.992	.008	80
50	.0054	.988	.012	45
60	.0047	.983	.017	30

Reference

Dames & Moore. Technical Support for GEIS: Radioactive Waste Isolation in Geologic Formations. Volume 21. Groundwater Movement and Nuclide Transport. Prepared for the U.S. Department of Energy. 1978. Y/OWI/TM-36/21.

7. HYDRAULIC CONDUCTIVITY OF FAULT ZONES

In the Task D Report, analyses of groundwater flow along pathways resulting from fault movement included an estimate of the hydraulic conductivity of the actual faulted pathway. Table 7-1 lists the estimated hydraulic conductivity values used in the Task D analyses. Recent hydrologic investigations of the Climax Stock granite at the Nevada Test Site have provided estimates of hydraulic conductivity for fractured zones in granitic rocks (Murray, 1981). Permeability tests of the Climax Stock at the Nevada Test Site yielded permeability values of 10^{-4} to 10^{-1} darcies for moderately to highly fractured rock. These values correspond to a hydraulic conductivity of 10^{-7} to 10^{-4} cm/s. Laboratory permeameter tests on material taken directly from fault shear zones and, therefore, representative of the hydraulic conductivity of the fault zone itself, yielded hydraulic conductivity values of 3×10^{-3} cm/s to 6×10^{-2} cm/s. On the basis of an analysis of the testing procedure, the investigations concluded that higher laboratory values, i.e., 6×10^{-2} cm/s, are probably more representative of field conditions than are the lower values. These higher values are in close agreement with those used for granite in the Task D analyses.

TABLE 7-1

HYDRAULIC CONDUCTIVITY OF FAULTED PATHWAYS USED IN THE TASK D REPORT

Rock Type	Hydraulic Conductivity cm/s
Bedded Salt	10^{-4}
Granite	10^{-2}
Basalt	10^{-2}
Shale	10^{-4}
Dome Salt	10^{-4}

Reference

Murray, W. A. Lawrence Livermore Laboratory. Geohydrology of the Climax Stock Granite and Surrounding Rock Formations, NTS. Prepared for the U.S. Department of Energy. May 1981. UCRL 53138.

8. HYDROLOGIC PARAMETERS FOR HOST ROCKS

8.1 REVIEW OF REFERENCE PARAMETERS

The Task C and D Reports each presented hydraulic conductivity and porosity values for various rock types, based on values reported in the literature. The purpose of this section is to compare these values and to supplement them with additional recent data. For hydraulic conductivity (also loosely referred to as "permeability" in some sources), this comparison is given in Figures 8-1 through 8-4. For porosity, a comparison is given in Table 8-1. Allowing for differences in the meaning of terms, e.g., total porosity vs. effective porosity, the original values are in good agreement and are confirmed by more recent results.

8.2 ASSUMPTION OF NEGLIGIBLE PERMEABILITY FOR SALT

There is support in the literature for the use of a zero value to characterize salt hydraulic conductivity for model calculations, although non-zero values have also been determined in a number of laboratory and in-situ tests. Higher values may be due in part to any or all of the following: disturbance of core samples by reduction of pressure, even if pressure is later reapplied; measurements with gases or organic liquids that do not lead to sealing of flow pathways; transmission of fluids into or through more permeable interbeds (as in measurements of hydrocarbon losses from storage cavities). Only the last of these is inherent to the salt deposit itself, and if the emphasis in modeling were on horizontal flow through the salt formation, then this factor might need to be considered. Vertical flow, which would lead to more rapid introduction of radionuclides into an aquifer, appears to be of greater concern, however, and the horizontal interbeds have little or no effect in transmitting water in this direction.

Several of the release mechanisms for a salt repository discussed in the Task D Report led to the calculation of volumetric flow rates for groundwater moving from the repository to the upper aquifer. In every case, the pathway for such flows was through some
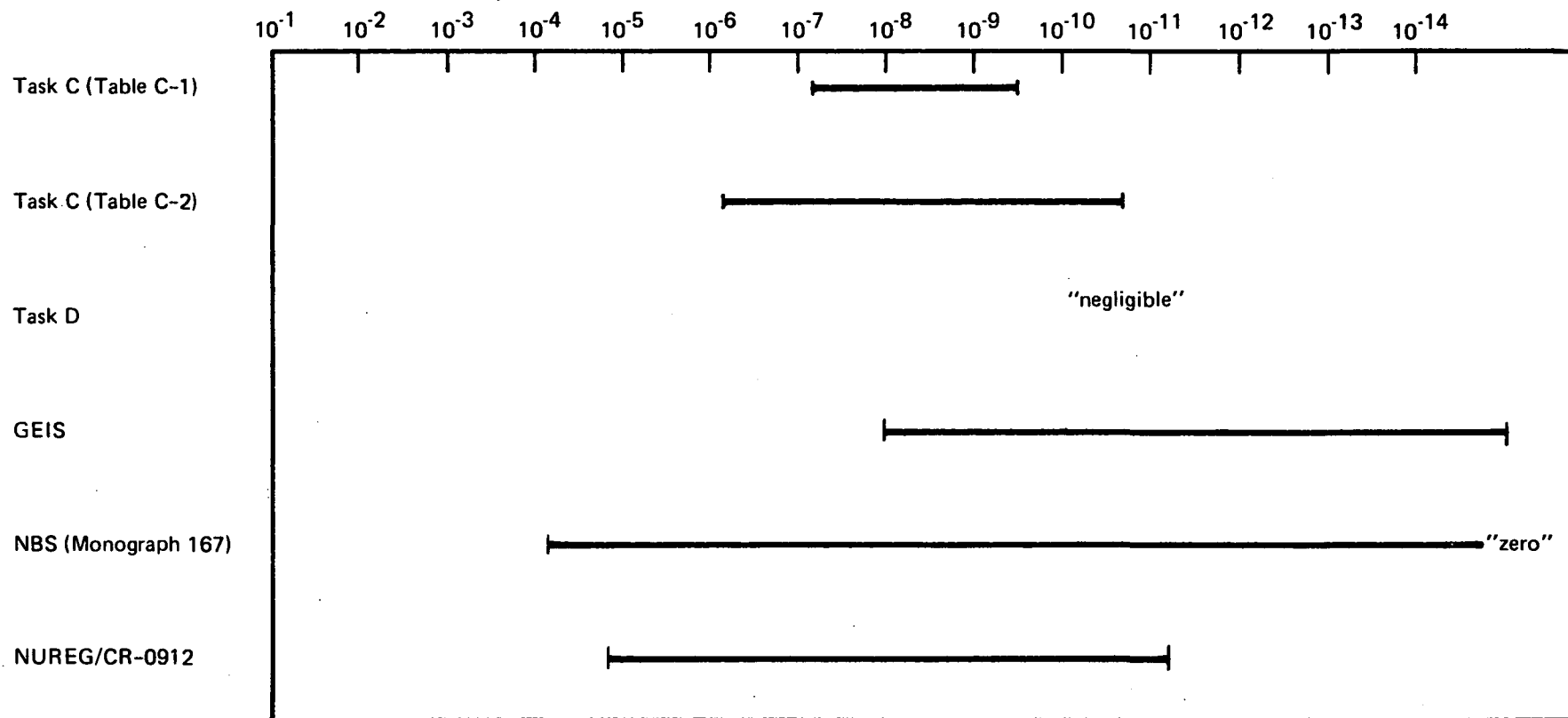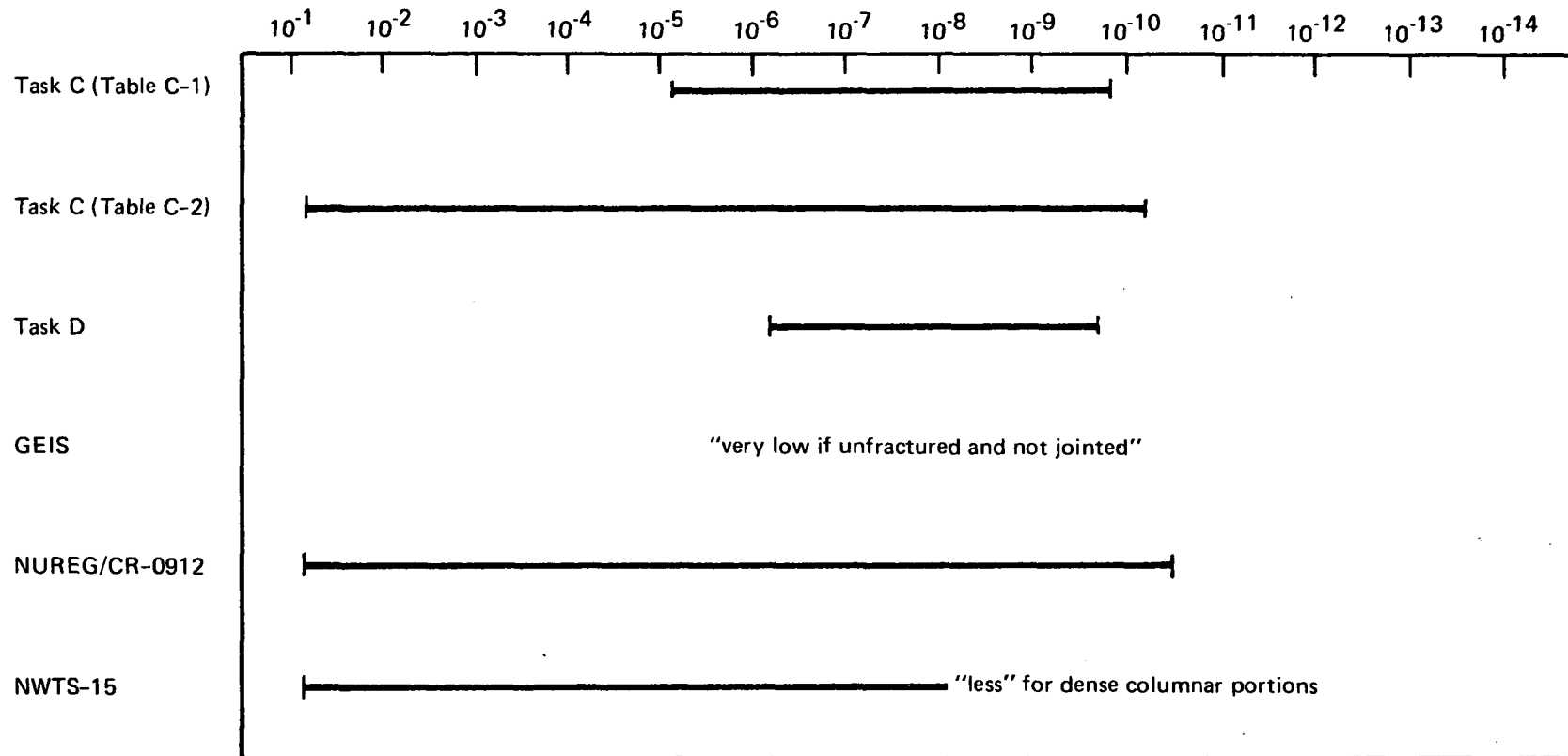
Note: For bibliographic citations, see the reference list at the end of Section 8.

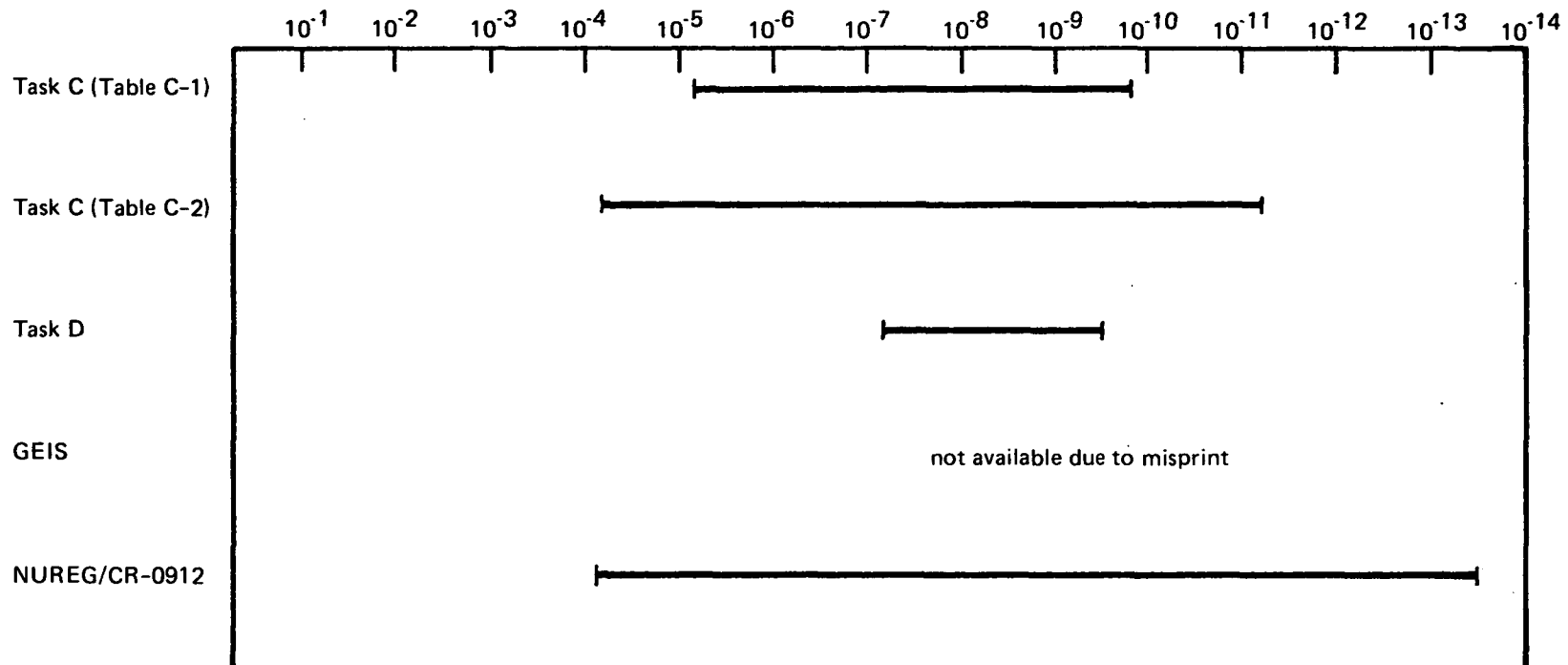FIGURE 8-1   REPORTED RANGES OR VALUES OF HYDRAULIC CONDUCTIVITY OF SALT (cm/sec)
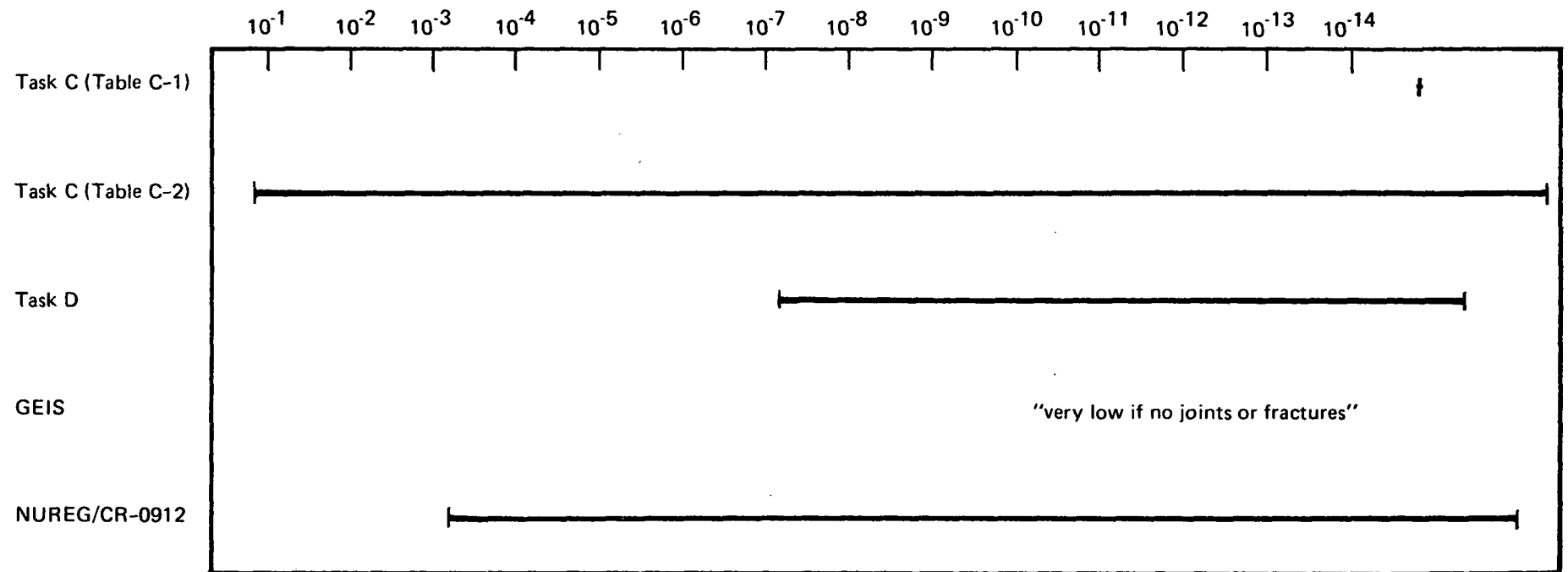
FIGURE 8-2   REPORTED RANGES OR VALUES OF HYDRAULIC CONDUCTIVITY OF GRANITE (cm/sec)

Note: For bibliographic citations, see the reference list at the end of Section 8.

Note: For bibliographic citations, see the reference list at the end of Section 8.

FIGURE 8-3   REPORTED RANGES OR VALUES OF HYDRAULIC CONDUCTIVITY OF BASALT (cm/sec)

Note: For bibliographic citations, see the reference list at the end of Section 8.

FIGURE 8-4   REPORTED RANGES OR VALUES OF HYDRAULIC CONDUCTIVITY OF SHALE (cm/sec)

65

TABLE 8-1

REPORTED RANGES OR VALUES OF POROSITY
OF POTENTIAL HOST ROCKS

Rock Type	Reference	Porosity	
Salt	Task C	< 0.01	
	Task D	none used	
	GEIS	0.014 - 0.10	
	NUREG	< 0.01	
	NBS	< 0.02	
Granite	Task C	0.06 - 0.09	
	Task D	0.001 - 0.0001	(fracture porosity)
	GEIS	0.005	
	NUREG	$5 \times 10^{-4} - 5 \times 10^{-6}$	(fracture porosity)
Basalt	Task C	0.03 - 0.04	
	Task D	0.001 - 0.0001	(fracture porosity)
	GEIS	0.006	
	NUREG	0.20 - 0.001	
Shale	Task C	0.03 - 0.07	
	Task D	0.001 - 0.0001	(fracture porosity)
	GEIS	0.0 - 0.45	
	NUREG	0.01 - 0.40	

anomalous feature, such as a partially sealed shaft or borehole, a fault, or a breccia column. (See especially Tables D-2, D-3, D-4, D-6, D-9, and D-10, of the Task D Report.) For the purpose of comparison, it is useful to calculate the Darcy flow through the entire repository itself, assuming some (small) positive hydraulic conductivity. Table 8-2 presents a set of representative values, based on a cross-sectional area of 8×10^6 m^2 for the flow path, i.e., the repository area. These flows are very small and indicate that flow through the bulk rock is generally not important in the case of salt.

8.3 VERTICAL FLOWS IN THE PRESENCE OF INTERBEDS FOR CASES OF BASALT AND SHALE

The generic repository setting for basalt was illustrated in Figure D-5 of the Task D Report and is repeated here as Figure 8-5. The basalt is shown to have a thickness of 200 meters. In fact, no single basalt flow in the Columbia River Basalt Sequence has such a thickness, and the generic basalt should be interpreted as a sequence of flows along with a number of interbeds. (This configuration is similar to the case of bedded salt, except that the interbeds in the basalt can be quite thick and rather permeable.) The purpose here is to calculate an equivalent hydraulic conductivity, K, for the composite vertical sequence, based on the characteristics of more than one type of layer. This is a straightforward calculation, but it is useful to have available both the formula and some representative results.

For simplicity, assume that the vertical flow pathway connecting the upper and lower aquifers through the repository consists of two basic types of material: dense basalt with hydraulic conductivity K_1 and more permeable zones (flow tops, interbeds) with hydraulic conductivity K_2. Let L_1 be the sum of the thicknesses of the dense basalt layers and L_2 the sum of the thicknesses of the other layers. Thus, for the generic repository setting,
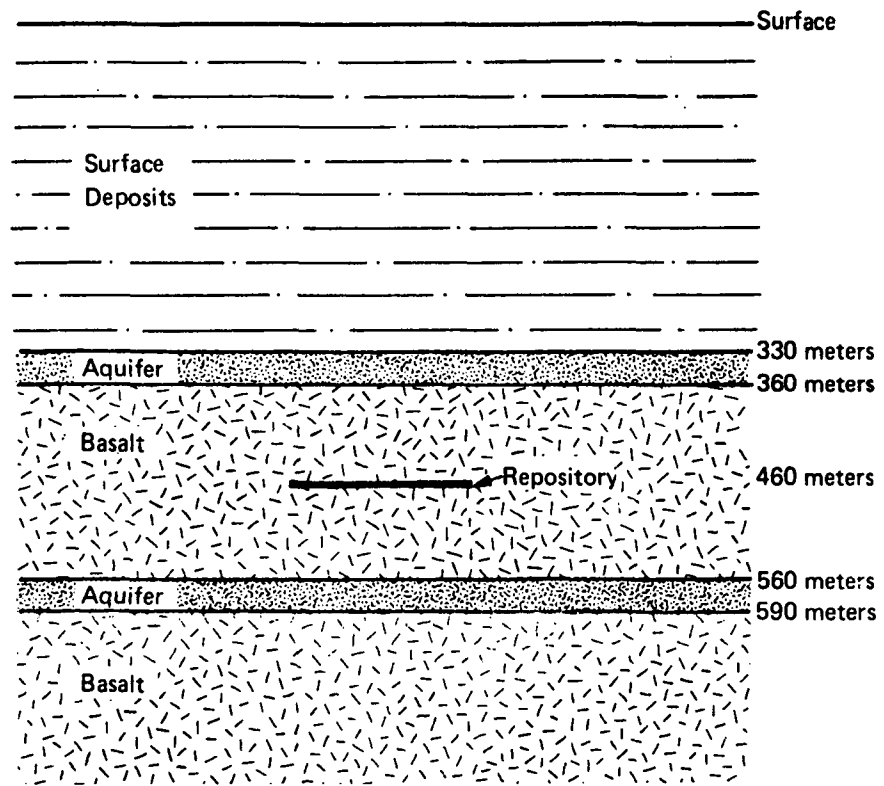
TABLE 8-2

VERTICAL VOLUMETRIC GROUNDWATER FLOWS THROUGH PORTION
OF SALT BED CONTAINING REPOSITORY, AS A FUNCTION OF
HYDRAULIC GRADIENT AND HYDRAULIC CONDUCTIVITY[*]

($\dot{Q}$ in m^3/yr)

Hydraulic Conductivity, K (cm/sec)	Hydraulic Gradient, i			
	0.001	0.01	0.02	0.1
10^{-14}	5×10^{-5}	5×10^{-4}	10^{-3}	5×10^{-3}
10^{-13}	5×10^{-4}	5×10^{-3}	10^{-2}	5×10^{-2}
10^{-12}	5×10^{-3}	5×10^{-2}	10^{-1}	5×10^{-1}
10^{-11}	5×10^{-2}	5×10^{-1}	1	5
10^{-10}	5×10^{-1}	5	10	50

[*]Note: Viscosity of water is assumed to be 0.005 poise, corresponding to an average temperature of 60°C. This would vary with time.

Surface

Surface
Deposits

Aquifer ········ 330 meters
········ 360 meters

Basalt

Repository 460 meters

Aquifer 560 meters
590 meters

Basalt

Source: Task D Report, Figure D-5.

FIGURE 8-5   GENERIC REPOSITORY IN BASALT

69

$$L_1 + L_2 = L = 200 \text{ m} \tag{8.1}$$

From the point of view of vertical flow calculations, the results are not affected by grouping the dense and permeable zones into two composite zones. Let A be the cross-sectional area of the vertical flow path. For the generic repository this would just be 8×10^6, the repository area. Let Δ_1 be the total head drop over the dense zones, and Δ_2 the drop over the permeable zones. By continuity of flow,

$$\dot{Q} = K_1 \frac{\Delta_1}{L_1} A\, c(\mu) = K_2 \frac{\Delta_2}{L_2} A\, c(\mu) \tag{8.2}$$

where Darcy's law (with viscosity correction) has been applied to each zone. The unknowns here are Δ_1 and Δ_2, the proportional drops over the two zones, and these are related by the additional equation

$$\Delta = \Delta_1 + \Delta_2 \tag{8.3}$$

It follows from solving the simultaneous equations that

$$\Delta_1 = \frac{\dfrac{L_1}{K_1 A}}{\dfrac{L_1}{K_1 A} + \dfrac{L_2}{K_2 A}}\, \Delta$$

$$\dot{Q} = \frac{\dfrac{L_2}{1}}{\dfrac{L_1}{K_1 A} + \dfrac{L_2}{K_2 A}}\, \Delta\, c(\mu)$$

$$= \frac{K_1 K_2 (L_1 + L_2)}{K_2 L_1 + K_1 L_2} \cdot \frac{\Delta}{L_1 + L_2} \cdot A\, c(\mu) \tag{8.4}$$

Comparing this with Darcy's law shows that the composite system has an effective conductivity given by

$$K = \frac{K_1 K_2 (L_1 + L_2)}{K_2 L_1 + K_1 L_2} \qquad (8.5)$$

Selected sample values are given in Table 8-3. These values illustrate that the low-permeability zone controls the flow, with essentially all the head drop taking place over it, i.e., $\Delta_1 \cong \Delta$. (This could also be deduced directly from the equation for K, or by considering an electrical resistance analogue.)

Suppose now that the dense zone has an effective porosity n_1 and the permeable zone an effective porosity n_2, where it is possible that n_2 is much larger than n_1. It is desired to calculate the average travel time of fluid as it passes through the flow pathway. The vertical linear velocity in the less permeable zone is given by

$$v_1 = \dot{Q}/n_1 A \qquad (8.6)$$

and in the more permeable zone by

$$v_2 = \dot{Q}/n_2 A \qquad (8.7)$$

The total travel time τ is the sum of the times in the two zones, given by

$$
\begin{aligned}
\tau &= \tau_1 + \tau_2 \\
&= \frac{L_1}{v_1} + \frac{L_2}{v_2} \\
&= \frac{L_1 \, n_1 A}{\dot{Q}} + \frac{L_2 n_2 A}{\dot{Q}} \qquad (8.8)
\end{aligned}
$$

TABLE 8-3

EQUIVALENT COMPOSITE HYDRAULIC CONDUCTIVITY OF FLOW PATH CONSISTING OF HIGHER AND LOWER PERMEABILITY ZONES
(cm/sec)

a) Higher Permeability Zones Equal to 50% Total Thickness

K_1 (Less Permeable Zone)	K_2 (More Permeable Zone)			
	10^{-6}	10^{-5}	10^{-4}	10^{-3}
10^{-9}	2×10^{-9}	2×10^{-9}	2×10^{-9}	2×10^{-9}
10^{-8}	2×10^{-8}	2×10^{-8}	2×10^{-8}	2×10^{-8}
10^{-7}	1.8×10^{-7}	2×19^{-7}	2×10^{-7}	2×10^{-7}
10^{-6}	10^{-6}	1.8×10^{-6}	2×10^{-6}	2×10^{-6}

b) Higher Permeability Zones Equal to 20% Total Thickness

K_1 (Less Permeable Zone)	K_2 (More Permeable Zone)			
	10^{-6}	10^{-5}	10^{-4}	10^{-3}
10^{-9}	1.2×10^{-9}	2×10^{-9}	2×10^{-9}	2×10^{-9}
10^{-8}	1.2×10^{-8}	2×10^{-8}	2×10^{-8}	2×10^{-8}
10^{-7}	1.2×10^{-7}	2×10^{-7}	2×10^{-7}	2×10^{-7}
10^{-6}	10^{-6}	1.2×10^{-6}	2×10^{-6}	2×10^{-6}

Thus if $L_2 n_2$ is much larger than $L_1 n_1$, which is quite likely, then the control on travel time is the more permeable and porous zone. In practice $L_2 n_2$ may be one or two orders of magnitude higher, the effect being to increase the fluid travel time significantly. Thus the following conclusion can be drawn:

> While the permeable zones have a relatively small effect in increasing volumetric flow rates, they can have a large effect in decreasing fluid velocities and hence increasing travel times.

For reference purposes, observe from Eq. (8.8) that

$$\tau = \frac{L_1 n_1 + L_2 n_2}{L_1 + L_2} \frac{(L_1 + L_2)A}{\dot{Q}} \qquad (8.9)$$

so that the effective porosity for velocity calculations is

$$\frac{L_1 n_1 + L_2 n_2}{L_1 + L_2}, \qquad (8.10)$$

which equals the average porosity. (Thus, porosity can be averaged while conductivity cannot.)

The same analysis applies to shale (and even to salt), but there are generally few or no significant interbeds in potential repository formations and so the results are not significant.

References

Lawrence Livermore Laboratory. Geoscience Data Base Handbook for Modeling a Nuclear Waste Repository. Volume I. Prepared for the U.S. Nuclear Regulatory Commission. January 1981. NUREG/CR-0912; UCRL-52719.

U.S. Department of Commerce. National Bureau of Standards (Gevantman, L. H., ed.), Physical Properties Data for Rock Salt. January 1981. NBS Monograph 167.

U.S. Department of Energy. Final Environmental Impact Statement. (GEIS). Management of Commercially Generated Radioactive Waste. October 1980. DOE/EIS-0046F.

U.S. Department of Energy. Proceedings of the 1981 National Waste Terminal Storage Program Information Meeting. November 1981. DOE/NWTS-15.

9. FRACTURE FLOW

The purpose of this section is to review the so-called "cubic law" for the hydraulic conductivity of fractured rock (based on unknown parallel fractures) and to survey various investigations that have tried to validate or modify it. This law was used in the Task C Report for certain calculations on flow through fractured rock. This model does appear to be valid for the generic calculations carried out.

Snow (1965) modeled flow in a fracture as flow between two smooth parallel plates. For a single fracture, the discharge is

$$\dot{Q} = \frac{ge^2}{12\upsilon} \frac{dh}{d\ell} (eW) \qquad (9.1)$$

where

$\dot{Q}$ = discharge of a fracture (cm^3/s)

e = fracture opening (cm)

g = gravitational acceleration constant (981 cm/s^2)

υ = coefficient of kinematic viscosity (0.013 cm^2/s for pure water at 10°C)

$dh/d\ell$ = head gradient (cm/cm)

W = width of the fracture (cm).

For a fracture of unit width, Eq. (9.1) becomes

$$\dot{Q} = \frac{ge^3}{12\upsilon} \frac{dh}{d\ell} \qquad (9.2)$$

This is the so-called cubic law for flow in fractures, and states that the discharge of a fracture is proportional to the cube of the fracture opening.

Darcy's law, adapted to evaluate the discharge from a single fracture, states:

$$\dot{Q} = KA \frac{dh}{d\ell} \tag{9.3}$$

By equating (9.1) and (9.3), and noting that $A = e \cdot 1 \text{ cm}^2$, an expression for the hydraulic conductivity of a single fracture can be developed:

$$K_f = \frac{ge^2}{12\nu} \tag{9.4}$$

The velocity in a single fracture is, then

$$v_f = \frac{ge^2}{12\nu} \frac{d\ell}{d\ell} \tag{9.5}$$

The effective hydraulic conductivity of a unit area of an array of parallel, evenly spaced smooth fractures of equal opening e, can be derived from Eq. (9.4), by multiplying K_f by the equivalent porosity of a unit area of material. This equivalent porosity can be written as the product of the area of a fracture per unit width of material and the number of fractures per unit length of material. This latter is equivalent to the inverse of the spacing between fractures. Thus, we have

$$K' = \frac{ge^3}{12\nu b} \tag{9.6}$$

where

b = spacing between fractures (cm) Hook and Bray (1974).
This expression is used in the Task C Report to describe the effective hydraulic conductivity of fractured rock. The velocity in a single fracture can be evaluated from Eq. (9.6) by dividing by the porosity, e/b, and multiplying by the head gradient, yielding Eq. (9.5).

The cubic law has formed the basis of theoretical investigations into fracture flow. Recent work has tended to confirm its validity, although extensions of the

theory to account for more realistic conditions have outstripped detailed experimental investigations. Louis and Maini (1970), Sharp et al. (1972), and Gale (1975) emphasized the concept of an "equivalent" aperture to account for fracture wall roughness and nonuniform flow, thus circumventing the difficulties of measuring roughness and nonuniform flow directly. While the calculation of effective fracture openings provides useful simplifications for modeling purposes, it has been noted that the approach produces values orders of magnitude smaller than actual measured openings (Gale, 1975). The relation of these differences to the actual velocities and transit times of fluid particles in a fracture _in situ_ has not been thoroughly explored. Witherspoon et al. (1980) studied the effects of cyclic loading of rough fractures in granite, basalt, and marble and found that deviations from the ideal parallel plate model could be accounted for by introducing a roughness factor, f, as a divisor in the flow equation, Eq. (9.2). Neuzil and Tracy (1981) extended the cubic law to the case of a fracture opening that varies continuously perpendicular to the flow but is uniform in the direction of the flow. They note the lack of suitable data from experimental work for testing the validity of current fracture flow theory.

Detailed physical description of fracture spacing and fracture openings is only one technique for measuring bulk conductivity. A given bulk conductivity value can result from a range of pairs of values of fracture opening and fracture spacing. Since the flow velocity in a fracture depends on the square of the opening, a small difference in fracture opening can significantly affect the time of first arrival of a particle of fluid or solute in the fluid. Furthermore, the parallel plate model analysis leads to a viscous flow with a maximum velocity 1.5 times the average velocity within a given fracture.

A range of fracture openings from 0.1 to 1000 μm is representative of the extremes of available data (Snow, 1968;

77

Witherspoon et al., 1980). Average velocities and times to travel 1 km, calculated for several values in the range, are shown in Table 9-1.

While there are few data available on fracture spacing and fracture aperture sizes at the depths being considered for repositories, data presented by Snow (1968) indicate fracture openings in the range of 50 - 100 μm at depths of 30 - 100 meters. It would be reasonable to expect smaller average values at greater depths, and consequently slower transit times.

TABLE 9-1

EFFECT OF APERTURE SIZE ON TRAVEL TIME

Fracture Opening (e), μm	Average Velocity (m/y)	Time to Travel 1 km (years)
0.1	2.0×10^{-3}	5.04×10^{5}
1.0	2.0×10^{-1}	5.04×10^{3}
10.0	2.0×10^{1}	5.04×10^{1}
100.0	2.0×10^{-3}	5.04×10^{-1}
1000.0	2.0×10^{5}	5.04×10^{-3}

Note: Values here are calculated using $\nu = 0.013$ cm^2/s, and a hydraulic gradient of 0.01 in Eq. (9.4).

References

Gale, J. A Numerical, Field, and Laboratory Study of Flow in Rocks with Deformable Fractures. University of California, Berkeley, Ph.D. dissertation. 1975.

Hook, E. and J. Bray. Rock Slope Engineering, Union Brothers, Ltd., England, 1974.

Louis, C. and Y. N. T. Maini. Determination of In-situ Hydraulic Parameters in Jointed Rock. In: Proc. 2nd Congress International Society for Rock Mechanics. Belgrade. 1, 1970.

Neuzil, C. E. and J. V. Tracy. Flow in Fractures. Water Resources Res., 17, 191-199, February 1981.

Sharp, J. C., Y. N. T. Maini, and T. R. Harper. Influence of Groundwater on the Stability of Rock Masses. Trans. Sec. A., Inst. Min. Metall. 81(782), A13, 1972.

Snow, D. T. A Parallel Plate Model of Permeable Fractured Media. University of California, Berkeley, Ph.D. dissertation. 1965.

_____ Rock Fracture Spacings, Openings, and Porosities. J. Soil Mech. Foundations Div. ASCE 94(5MI), 73. 1968.

Witherspoon, P. A., J. S. Y. Wang, K. Iwai, and J. Gale. Validity of Cubic Law for Fluid Flow in a Deformable Rock Fracture. Water Resources Research 16, 1016-1024, December 1980.

10. GEOCHEMICAL RETARDATION

The purpose of this section is to update the retardation factors reported earlier in the Task C Report.

Geochemical retardation affects radionuclide transport by causing ions to move at velocities lower than that of the transporting groundwater. The retardation factor is a measure of the ratio of the velocity of the flowing groundwater to that of the radionuclide under consideration and represents the sorptive capacities of the geologic medium. The sorptive capacity is represented by a distribution coefficient that reflects the partitioning of the radionuclide between the groundwater and the solid part of the medium. The retardation factor is usually calculated on the basis of the physical properties of the medium together with the distribution coefficient, or it is measured in the field or laboratory using pulse tracer tests.

The retardation factor (R_d) is related to the distribution coefficients by the following relationships:

For porous media, $R_d = 1 + \frac{\rho}{\phi} K_d$ (dimensionless) (10.1)

For fractured media, $R_d = 1 + R_f K_a$ (dimensionless) (10.2)

where

ρ = bulk density of the medium (g/cm^3)

ϕ = porosity

R_f = surface to volume ratio of the fracture (cm^2/ml)

K_d, K_a = distribution coefficients for porous and fractured media, respectively.

If there is no sorption, the distribution coefficients are zero and the retardation factors take their minimum value ($R_d = 1$). Figure 10-1 shows the relationship between the retardation factor and the distribution coefficient for two porous rock media.
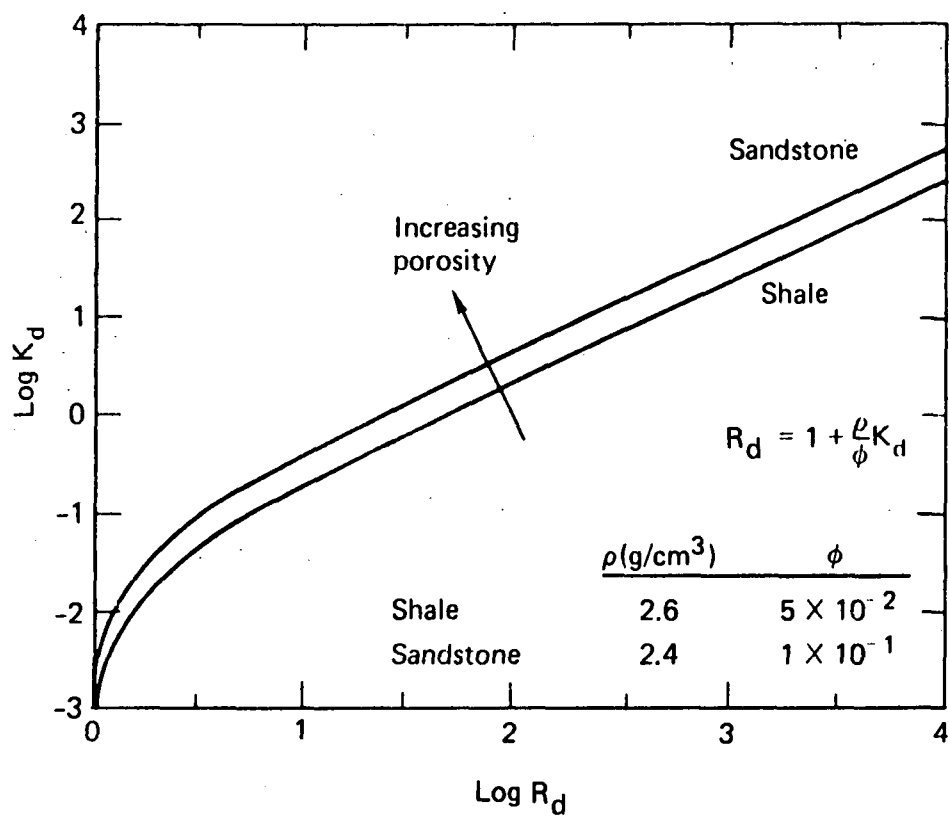
Source: Adapted from NUREG/CR 0912, 1981.

FIGURE 10-1   RELATIONSHIP BETWEEN RETARDATION FACTOR, R_d, AND DISTRIBUTION COEFFICIENT, K_d

Measurements of density, porosity, and distribution coefficients are easily made in the laboratory, but it is not known how well the laboratory measurements of K_d represent field conditions. Thus, it is uncertain how well the calculated retardation factors represent field conditions.
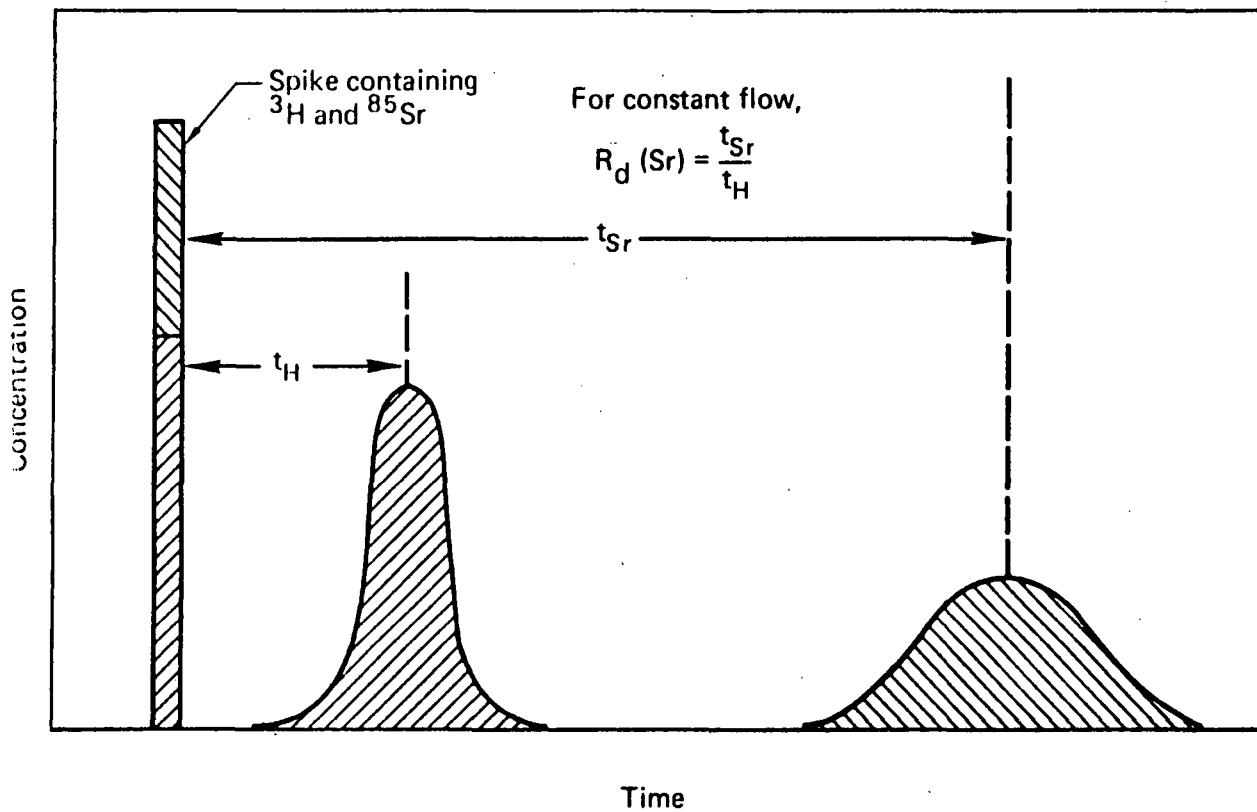
10.1 FIELD MEASUREMENTS OF RETARDATION FACTOR

Field measurements of retardation factors are commonly made by trace injection tests. Radionuclides are injected into groundwater at one well and measured at a second well some distance away. The in-situ retardation factors are calculated by dividing the travel time of each radionuclide by the travel time for tritium (a nonreactive tracer) as shown in Figure 10-2.

In-situ measurements of retardation factors are generally more reliable than those based on laboratory measurements because they are representative of the local geologic environment, taking into account the heterogeneity of the geologic material. The effects of such parameters as temperature, oxidation potential, and pH cannot be determined, however, because these factors are generally constant in the field environment. Data from in-situ measurement of radionuclide migration in deep groundwater are limited and are summarized in Table 10-1.

10.2 CALCULATED RETARDATION FACTORS BASED ON DISTRIBUTION COEFFICIENTS

Figure 10-3 is an updated version of Figure C-1 of the Task C Report. This figure was modified to include more current information regarding distribution coefficients for strontium and cesium. The new information was contained in a report prepared for the U.S. Nuclear Regulatory Commission by Muller et al. (1981).

Table 10-2 was prepared from information contained in the Lawrence Livermore report (1981) and summarizes the range of retardation factors estimated from distribution coefficients compiled from the literature. The table is subdivided into three major groups: fission products with no sorption, fission products

Source: Adapted from NUREG/CR 0912, 1981.

FIGURE 10-2   ILLUSTRATION OF CALCULATION OF R_d FROM IN-SITU MEASUREMENT OF TRAVEL TIMES BETWEEN TWO WELLS
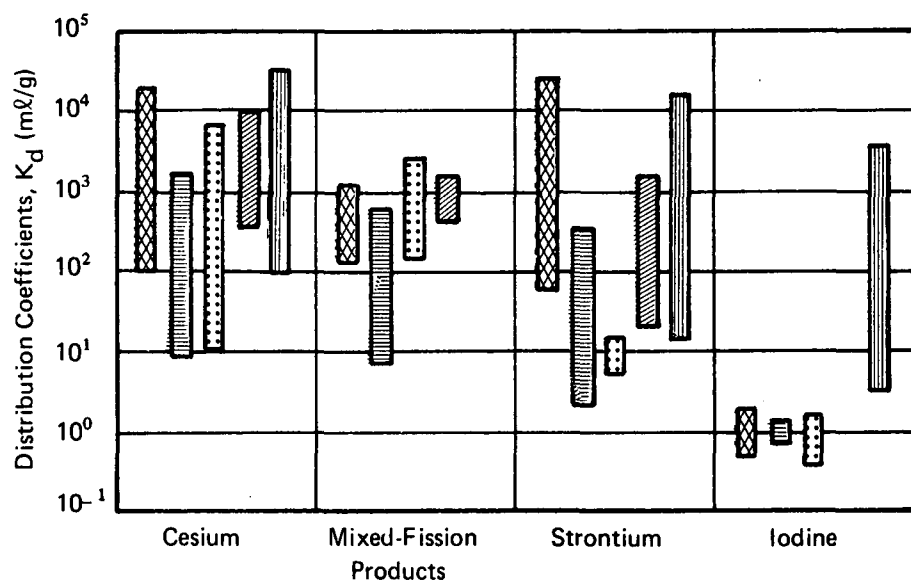
TABLE 10-1

RETARDATION FACTORS BASED ON IN-SITU MEASUREMENTS

OF RADIONUCLIDE MIGRATION IN DEEP GROUNDWATER

	Strontium	Cesium	Technetium	Iodine	Neodymium
Basalt[1]	4	NMD*	-	-	-
Granite[2]	6	NMD*	1	1	NMD*

[1]Robertson and Barraclough, 1973
[2]Landstrom et al., 1979
*No migration detected

Note: Distribution coefficient values for ions shown.

Sources: SAND81—0557 and BNWL—1900.

Legend:

▨	Tuff
▤	Granite
⬚	Limestone and Dolomite
▨	Basalt
▥	Soils

FIGURE 10-3   RANGES OF DISTRIBUTION COEFFICIENTS FOR VARIOUS ROCK TYPES

TABLE 10-2

REPRESENTATIVE RETARDATION FACTORS*

	Retardation Factor
<u>Fission products with no sorption</u>	
Iodine and technetium	1
<u>Fission products with sorption</u>	
Strontium	100 (for dilute groundwater;
Cesium	> 100 substantially smaller
	for brines)
<u>Actinides and daughter products</u>	
Thorium ⎫	
Plutonium ⎪	
Americium ⎬	100 - 100,000
Neptunium ⎪	
Radium ⎭	

*Based on laboratory measurements of distribution coefficients and applicable for modeling a generic repository.

Source: Adapted from NUREG/CR-0912.

with sorption, and actinides and their daughter products. As there was a considerable range of distribution coefficients listed for each of the radionuclides within each group, representative retardation factors, applicable to generic repository model analyses, were tabulated.

Experimental evidence has shown that retardation factors are, in part, functions of rock types, pH, water composition, and flow rates, but the interrelationships among these parameters and their effect on retardation are largely unknown. Until laboratory experiments are correlated with in-situ conditions, considerable uncertainty may be expected in the results of analyses of radionuclide transport (Lawrence Livermore Laboratory, 1981).

References

Landstrom, O., C. Klockars, K. Holmberg, and S. Westerberg. In-situ Experiments on Nuclide Migration in Fractured Crystalline Rocks. Proc. Symposium on Science Underlying Radioactive Waste Management. (Materials Research Society). 1979.

Lawrence Livermore Laboratory. Geoscience Data Base Handbook for Modeling a Nuclear Waste Repository. Volume I. Prepared for the U.S. Nuclear Regulatory Commission. January 1981. NUREG/CR-0912.

Muller, A. B., N. C. Finley and F. J. Pearson, Jr. Geochemical Parameters Used in the Bedded Salt Reference Repository Risk Assessment Methodology. Sandia National Laboratories. Prepared for the U.S. Nuclear Regulatory Commission. September 1981. SAND-81-0557; NUREG/CR 1996.

Robertson, J. and J. Barraclough. Radioactive and Chemical Waste Transport in Groundwater at National Reactor Testing Station, Idaho: 20 Years Case History and Digital Model, in Underground Waste Management and Artificial Recharge. (J. Brownstein, ed.) Am. Assoc. Petrol. Geol. 1, p. 291-332. Minasha, Wisconsin, George Banta Co., 1973.

Schneider, K. J. and A. M. Platt (eds.). High-Level Waste Management Alternatives. BNWL 1900, Battelle Pacific Northwest Laboratories, Richland, Washington. May 1974.